

See discussions, stats, and author profiles for this publication at: <https://www.researchgate.net/publication/230531047>

Nonlinear impacts of climatic variability on the density-dependent regulation of an insect vector of disease

Article in *Global Change Biology* · September 2011

DOI: 10.1111/j.1365-2486.2011.02522.x

CITATIONS

80

READS

209

4 authors, including:



Luis Fernando Chaves

Costa Rican Institute for Research and Education on Nutrition and Health

235 PUBLICATIONS 4,925 CITATIONS

[SEE PROFILE](#)



Amy C Morrison

University of California, Davis

401 PUBLICATIONS 8,761 CITATIONS

[SEE PROFILE](#)

Some of the authors of this publication are also working on these related projects:



influenza & Other respiratory virus [View project](#)



SENACYT COL-11-043 [View project](#)

Nonlinear impacts of climatic variability on the density-dependent regulation of an insect vector of disease

LUIS F. CHAVES*†, AMY C. MORRISON‡, URIEL D. KITRON§¶ and THOMAS W. SCOTT‡¶

*Graduate School of Environmental Sciences & Global Center of Excellence Program on Integrated Field Environmental Science, Hokkaido University, Sapporo 060-0810, Japan, †Programa de Investigación en Enfermedades Tropicales, Escuela de Medicina Veterinaria, Universidad Nacional, PO Box 304-3000, Heredia, Costa Rica, ‡Department of Entomology, University of California, Davis, CA 95616 USA, §Department of Environmental Studies, Emory University, Atlanta, GA 30322 USA, ¶Fogarty International Center, National Institutes of Health, Bethesda, MD 20892 USA

Abstract

Aedes aegypti is one of the most common urban tropical mosquito species and an important vector of dengue, chikungunya, and yellow fever viruses. It is also an organism with a complex life history where larval stages are aquatic and adults are terrestrial. This ontogenetic niche shift could shape the density-dependent regulation of this and other mosquito species, because events that occur during the larval stages impact adult densities. Herein, we present results from simple density-dependent mathematical models fitted using maximum likelihood methods to weekly time series data from Puerto Rico and Thailand. Density-dependent regulation was strong in both populations. Analysis of climatic forcing indicated that populations were more sensitive to climatic variables with low kurtosis, i.e., climatic factors highly variable around the median, rainfall in Puerto Rico, and temperature in Thailand. Changes in environmental variability appear to drive sharp changes in the abundance of mosquitoes. The identification of density-independent (i.e., exogenous) variables forcing sharp changes in disease vector populations using the exogenous factors statistical properties, such as kurtosis, could be useful to assess the impacts of changing climate patterns on the transmission of vector-borne diseases.

Keywords: *Aedes aegypti*, climate change, exogenous forcing, kurtosis, modeling, mosquito, population regulation, Schmalhausen's law

Received 17 May 2011 and accepted 6 August 2011

Introduction

Aedes aegypti (L.) (Diptera: Culicidae) is a common pantropical urban mosquito with a complex life cycle and vector of several human pathogens. In general, the complex life cycle of mosquitoes is driven by a major ontogenetic niche shift between larval and adult stages. *Ae. aegypti* larvae inhabit aquatic habitats and forage on suspended particles and aquatic organisms (Christophers, 1960), terrestrial adults fly, and primarily forage on plant sugars or blood for female egg development (Harrington *et al.*, 2001). The success of *Ae. aegypti* in urban environments is due to the abundance and suitability of larval habitats, i.e., artificial water containers, and resources for reproduction, such as blood from human hosts (Edman, 1988). These characteristics and other behavioral aspects make this mosquito a very efficient vector of several pathogens (Gubler, 1989), most notably, dengue, chikungunya, and yellow fever viruses. Complex life cycles represent a major challenge to understand density-dependent regulation of popula-

tions (Ratikainen *et al.*, 2008). For example, density-dependent regulation during larval stages has been proposed as a major determinant of *Ae. aegypti* adult population size (Dye, 1984). However, the impact of exogenous factors, such as resource limitation, can also regulate the abundance of adult mosquitoes (Legros *et al.*, 2009). An additional layer of complexity is added by the sensitivity of *Ae. aegypti* populations to changes in the external environment. For example, eggs diapause and only hatch when humidity is very high or after they become submerged in water, and like other insects, their developmental rate is a function of temperature (Christophers, 1960). Trying to understand the combined effect of all these factors in shaping the abundance of *Ae. aegypti* has been primarily tackled with complex models that capture a large quantity of biologic details (Gilpin & McClelland, 1979; Focks *et al.*, 1993; Magori *et al.*, 2009). Such models, although capable of replicating some real scenarios, lack the power to offer generalizations about the processes regulating population dynamics and tend to ignore the role of the changing environment (Levins, 1968). Thus, understanding the canalization of environmental variability on population dynamics, where environmental changes

Correspondence: Luis Fernando Chaves, tel. + 81 11 706 2267, fax + 81 11 706 4954, e-mail: lchaves@ees.hokudai.ac.jp

impacting the development of organisms have the power to shift their population dynamics (Schmalhausen, 1949), becomes both an interesting question and a pressing need to be prepared against societal challenges that might emerge from the response of living organisms to climate change (Chaves & Koenraadt, 2010).

Herein, we use simple models to understand the importance of exogenous climatic factors, i.e., forcing, and density dependence on *Ae. aegypti* population dynamics. We ask whether population dynamics of this mosquito species can be forced by climatic factors, when density-dependent regulation is considered, and whether it is possible to predict which climatic factor is most likely to force the dynamics based on the distribution moments of the considered climatic variables. We ask these questions based on the corollary of Schmalhausen's Law, which predicts that organisms can be more sensitive to extreme events in variables where conditions around the median are more uncertain (Chaves & Koenraadt, 2010). Our goal is to derive generalizations about the canalization of climatic variability on population dynamics of this mosquito species, a prototype of organisms with complex life cycles. We use maximum likelihood methods to fit data from weekly time series of domiciliary mosquito abundance from Puerto Rico and Thailand (Scott *et al.*, 2000) to simple mathematical models with density-dependent recruitment of adult individuals. We use nonlinear functions to incorporate the impacts of rainfall and temperature on mosquito population dynamics, and to successfully capture the nonstationary impacts of climatic variability on the dynamics of both populations unveiled using cross-wavelet analysis. Our results show that density-dependent regulation of adult individuals is present in populations at both locations. Parameter estimates and mathematical analysis of the best model support density-dependent dynamics with a single stable nontrivial equilibrium, where any response to perturbations is expected to be transient. However, population dynamics can be reactive, transiently altering population densities via propagation of disturbances, especially when immature survival is low and fecundity is high. In fact, the product of these parameters, immature survival and fecundity, is of major importance to the dynamics of the populations we studied, as revealed by a perturbation analysis of the best model with parameter estimates from the best fits. Populations are more sensitive to small changes in climatic variables with a relative wider variability around the median (a platykurtic variability); i.e., rainfall for Puerto Rico and temperature for Thailand. This result shows the importance of climatic variability on population dynamics, a topic rarely explored in the context of the forcing of population dynamics, where the main focus has been on the impact

of average values (Pascual *et al.*, 2006). Our results also highlight aspects of the internal relations between climate change and climate variability (Stenseth *et al.*, 2002; Paaijmans *et al.*, 2010) by stressing the importance that changes in the variability of climate, especially the frequency of extreme events, can have on the population dynamics of organisms.

Materials and methods

Data

Weekly mosquito density time series data (Fig. 1) were obtained by averaging *Ae. aegypti* abundance obtained from 10 houses (out of a total of 36 monitored houses) in the neighborhoods of Reparto Metropolitano and Puerto Nuevo, Rio Piedras (18°23'N, 66°39'W) Puerto Rico; and from 10 houses (out of a total of 23 monitored houses) in Village 6 (13°38'N, 101°18'E) of Hua Sam Rong Tambon (subdistrict), Plaeng Yao Amphoe (county), Chachoengsao (province) in Thailand. In both sites, none of the houses was sampled in consecutive weeks. Houses were sampled using a battery powered aspirator in Puerto Rico (March 1991–March 1993) and modified vacuum cleaners in Thailand (June 1990–May 1993). These are reliable and comparable methods for sampling adult *Ae. aegypti* populations (Scott *et al.*, 2000). Samples were restricted to houses because this is the main resting habitat of adult *Ae. aegypti* (Christophers, 1960; Scott *et al.*, 2000). Temperature and rainfall records (Fig. 1) were obtained from weather stations within a 20 KM radius of the sampled sites. Seasonal patterns of rainfall and temperature range in Puerto Rico and Thailand, during the respective study periods, were within the range of recorded variability for the studied areas (Fig. S1). See Scott *et al.* (2000) for further details on study sites, sampling, and time series data.

Descriptive time series analysis

We examined the correlation structure of mosquito time series data using standard techniques for time series analysis (Shumway & Stoffer, 2000). These included the autocorrelation function (ACF), the Partial ACF (PACF), and the cross-correlation function (CCF) of the pre-whitened residuals. We also assessed the nonstationary patterns of association (i.e., changing through time) between climatic variability and mosquito time series using cross-wavelet analysis (Chaves & Pascual, 2006; Cazelles *et al.*, 2007). We used this information to verify assumptions considered in the process of model building. Further details are presented in the Appendix.

Description of the variability in the climatic time series

Rainfall and temperature are very different phenomena, both in terms of the physical variables measured, their dynamics, and how they are recorded. Rainfall is episodic (i.e., at any time it either rains or not) and records of rainfall are cumulative (i.e., a time series of rainfall shows the cumulative amount of rain in place for a time period). In contrast, temperature con-

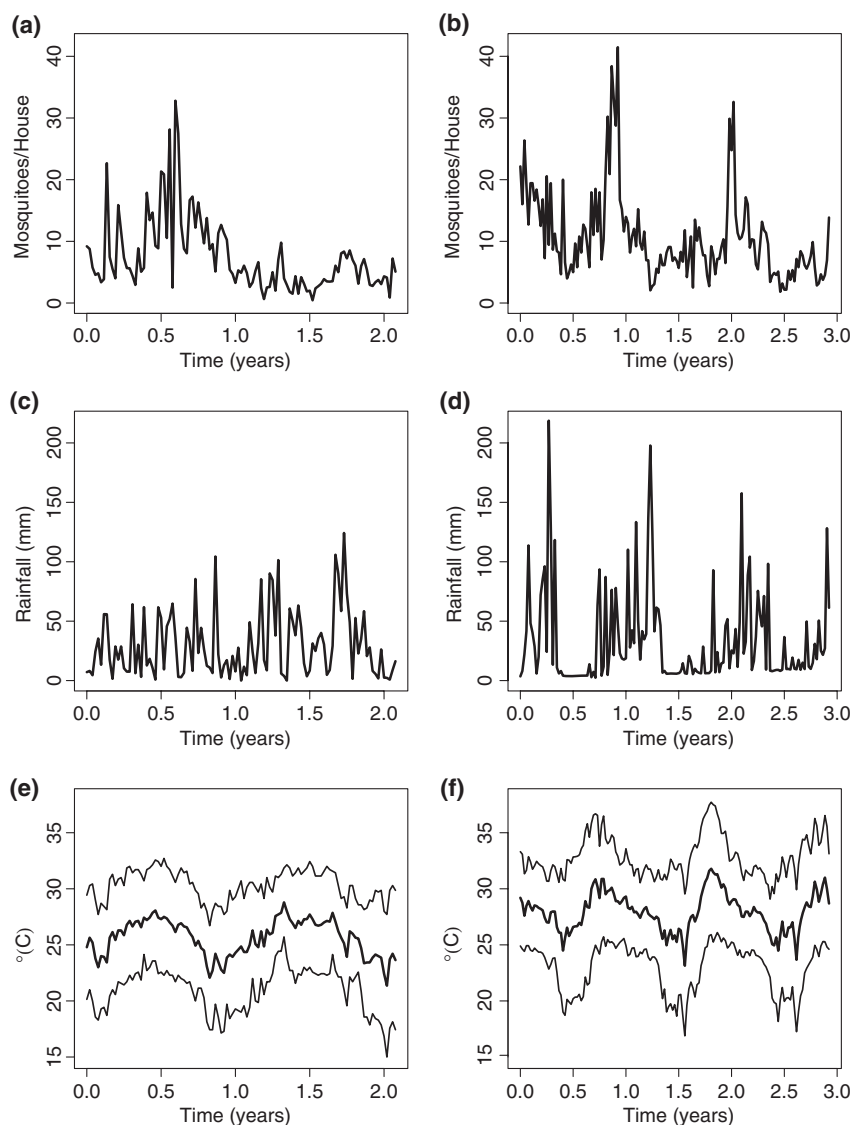


Fig. 1 Data. Weekly average mosquito density per house, N_t , in (a) Puerto Rico and (b) Thailand; cumulative weekly rainfall in (c) Puerto Rico and (d) Thailand; weekly temperature average, thick line, maximum and minimum, thin lines, in (e) Puerto Rico and (f) Thailand.

stantly fluctuates, and the way in which it is recorded includes point measurements that normally are averaged over a time period, and for those time periods, maximum and minimum can be recorded. These differences make the standardization of records necessary to make them comparable. A common procedure to standardize rainfall variability is to accumulate values over time and keep the residuals of a linear regression of these accumulated values as function of time (Pascual *et al.*, 2008). In the case of temperature, living organisms experience all the different values occurring during a time period. As *Ae. aegypti* is known to be sensitive to extreme temperature values (Headlee, 1940; Bar-Zeev, 1958a) we computed the range of the weekly temperatures to study variability.

An additional challenge in depicting variability in climatic factors is describing the kind of variability experienced by individuals. For example, variance will give an idea of the var-

iability around the mean value, which can be standardized to the magnitude of the mean by computing the coefficient of variation; i.e., the ratio between the standard deviation and the mean. However, according to Schmalhausen's law (Chaves & Koenraadt, 2010), organisms normally cope with regular patterns of variability and can be differentially sensitive to extreme events, depending on how common or infrequent these extreme events are. However, variance and the coefficient of variation fail to provide information about the frequency of events close and far from the mean. To study the variability in the environmental factors, we used the kurtosis, also known as the fourth standardized moment, which measures how much of the variability in a distribution is due to infrequent extreme events as opposed to modestly sized deviation from the mean (Mardia, 1970). Mathematically, kurtosis, K , is defined as the ratio between the fourth

moment around the mean, μ_4 , and the square of the variance, σ^2 , i.e., $K = \mu_4/\sigma^4$ (Mardia, 1970).

Models: structure, data fitting and selection

We considered three models: (1) Delayed Ricker, (2) Delayed Beverton-Holt, and (3) Delayed Gompertz, to select the model with the highest ability to explain the observed mosquito records. The Delayed Ricker model comes from the discrete time integration of the delayed logistic equation (Turchin, 2003), and the Delayed Beverton-Holt and Gompertz models abstract the processes whereby the population size at a given time is a function of survivors from the previous time step and the recruitment of emerging adults whose density is a nonlinear function of the 2-week lagged adult density. These mechanisms seem appropriate to describe the dynamics of *Ae. aegypti*, because for the recorded temperatures at our study sites, the pre-imaginal developmental roughly corresponds to a week (Headlee, 1940). *Ae. aegypti* larval density, similarly, does not seem to affect adult emergence success when resources are not limiting (Bar-Zeev, 1957; Wada, 1965; Barbosa *et al.*, 1972; Dye, 1982). However, emerging individuals are smaller and less fecund (Bar-Zeev, 1957). We fitted the mosquito time series to these models considering all possible combinations of the following cases: (1) Both with and without considering exogenous forcing, EXO, using nonlinear functions that allowed us to test the existence of climatic forcing on *Ae. aegypti* population dynamics, (2) Assuming that the impact of the forcing was either multiplicative or additive, to test whether the forcing acted on the rate of population growth, i.e., a multiplicative forcing, or had mere additive effects (Stenseth *et al.*, 2002), and (3) Considering either observation error or environmental stochasticity, to assess whether unexplained factors homogeneously affected all individuals, as expected under environmental stochasticity (Mangel, 2006), or more likely represented systematic errors in our records (Bolker, 2008). We considered that errors had a normal distribution and fitted the models using maximum likelihood methods (Bolker, 2008). We then selected the best models for each site using the Akaike and Bayes Information Criteria (Shumway & Stoffer, 2000). Full details about the models, detailed assumptions, equations (including a stage structured matrix representation of the best model), and nonlinear functions for the exogenous forcing and maximum likelihood parameter estimation are presented in the Appendix.

Stability, reactivity and perturbation analysis of the best models

For each of the best models per study site, both with and without exogenous forcing, we performed a stability analysis to determine the conditions for persistence of the population with the estimated parameters (Levins & Wilson, 1980). We tested the significance of the stability by performing a bootstrap as described by Neubert *et al.* (2009). We also studied the reactivity of the system; i.e., the maximum amplification rate of a perturbation immediately after its occurrence (Neubert *et al.*, 2009), and generated a map for reactive parameter

regions. A reactivity analysis helps to further understand the transient dynamics of a stable population when perturbed away from its equilibrium. In the case of *Ae. aegypti*, the reactivity analysis provides insights on the role that its stage structure could have in transient mosquito outbreaks. Furthermore, model derivation and parameter constraints made possible a reactivity analysis in absence of larval data (see Appendix for further details, especially regarding the connections between discrete time equations and stage structured matrix models). We also performed a perturbation analysis consisting of sensitivity and elasticity analyses, which quantitate the impacts of changes in parameters in absolute and in relative terms, respectively. For the perturbation analysis, we used methods recently developed for nonlinear systems described by Caswell (2008). Full details about the analytic and computational procedures are presented in the Appendix.

Results

To examine the structure of the mosquito density time series and its linear association with climatic variables, we performed a descriptive time domain analysis for each time series (Shumway & Stoffer, 2000). We used each mosquito time series to compute ACF, PACF, and CCF functions with the pre-whitened time series of the climatic variables (Fig. S2). We found both time series to be second order autoregressive processes (Fig. S2b and d). The Puerto Rico time series was positively associated with a 1-week lagged rainfall (Fig. S2e), and the Thai time series was positively led by maximum temperature with a lag of 10 weeks (Fig. S2k). To further confirm this association, we used cross-wavelet coherence and phase analyses in the time-frequency domain (Cazelles *et al.*, 2008). This analysis confirmed the association between the climatic and mosquito time series, and showed the association to be nonstationary (Fig. S3) as demonstrated by the lack of a continuous coherence in the time-frequency domain, i.e., the association changed in strength and significance over time, especially with rainfall in Puerto Rico (Fig. S3a top plot), and with maximum temperature in Thailand (Fig. S3g top plot). Regarding the cross-wavelet phase, it is important to highlight that angles separating mosquito abundance, N_t , and rainfall in Puerto Rico (Fig. S3a bottom plot) and N_t and maximum temperature in Thailand (Fig. S3g bottom plot) were positive, indicating that peaks in mosquito abundance follow peaks in the forcing variables considered in the models, robustly supporting the patterns observed with the cross-correlation functions (Fig. S2e and k). This information was used to define nonlinear functions for the forcing able to capture the nonstationary associations, as explained in detail in the Appendix. To evaluate the potential for density dependence, we plotted the per-capita growth rate, r , of each series as a function of current density,

N_t , and 1 week of lag density, N_{t-1} , and found that in both mosquito time series, the values of r decrease when both densities are high, and increase when both densities are low (Fig. 2a and b). To further understand the impacts of the forcing, we plotted density, N_t , as function of environmental covariates (Fig. 2c and d). For Puerto Rico, the relationship between mosquito abundance and rainfall was best described by the absolute difference in rainfall for two consecutive weeks, where low mosquito densities are associated with highly variable rainfall (Fig. 2c). For Thailand the relationship between mosquito abundance and maximum temperature showed a positive association when values were above a threshold value of ca. 34 °C (Fig. 2d). The Akaike and Bayes information criteria (Table S1) selected the Gompertz model with environmental stochasticity as the best model to describe the density-dependent regulation of both mosquito populations:

$$N_t = (sN_{t-1} + p(\lambda N_{t-2}^\theta)) \exp(\varepsilon) \quad (1)$$

In this model, s denotes adult survival, p the emergence probability of immature mosquitoes, λ the per-capita fecundity, θ is an exponent that accounts for density dependence, and ε is a random, independent, and identical distributed normal variable with variance σ_{envs}^2 . Further details and assumptions of this model

and its derivation from a stage-structured model are presented in the Appendix. The model in equation (1) increased the amount of deviance explained when compared with a 2nd order autoregressive model, over 62% vs less than 20% (Scott *et al.*, 2000), and more deviance was explained when the forcing through simple additive functions, $EXO(\text{ClimaticVariable})$, was included:

$$N_t = (sN_{t-1} + p(\lambda N_{t-2}^\theta) + EXO(\text{ClimaticVariable})) \exp(\varepsilon) \quad (2)$$

In the case of Puerto Rico, the forcing by rainfall was included using a saturation function. In the case of Thailand, forcing by the maximum temperature was included using a threshold function (see Materials and methods and Appendix). Due to parameter unidentifiability between p and λ in equations (1) and (2), which arises from the transformation of a stage-structured matrix model into a delayed difference equation (for details see the Appendix), we only estimated $\lambda' = p\lambda$. We estimated parameters for the models with and without forcing for Puerto Rico and Thailand (Table 1). Interestingly, the variables that increased the likelihood when considered for forcing had the lowest kurtosis; i.e., their variability was wide around the median (Fig. 3a and b). This result might indicate an increased sensibility of mosquitoes to small changes in environ-

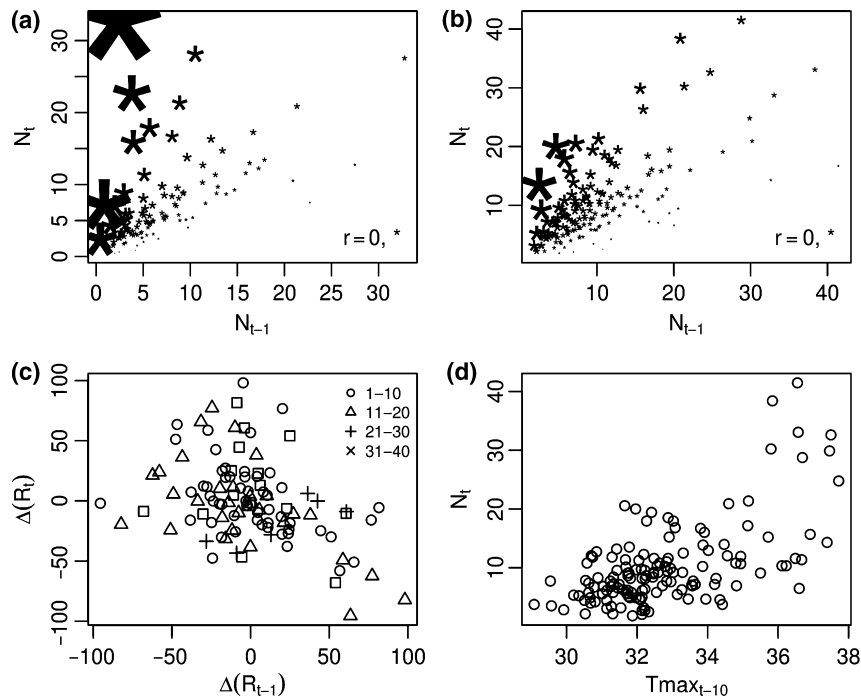


Fig. 2 Density Dependence and Forcing. Population growth rate [$r = \log N_t - \log N_{t-1}$, represented by * in the plots] as function of current [N_t] and 1 week of lag [N_{t-1}] densities in (a) Puerto Rico and (b) Thailand. *size is proportional to the growth rate (see legend for reference when $r = 0$) (c) Puerto Rico current density [N_t] as function of two lags in the difference of rainfall, ΔR . The legend indicates different ranges of N_t (d) Thai current density [N_t] as function of maximum temperature, T , with 10 weeks of lag.

Table 1 Parameter estimates and confidence limits of the best models for Thailand and Puerto Rico. In both sites, the Gompertz model was best. In Thailand, the forcing was via a threshold function of maximum temperature with a lag of 10 weeks. In Puerto Rico, the forcing was via a Holling type II saturating function of rainfall, in which the numerator had a lag of 1 week and the denominator had a lag of 2 weeks. Details about the forcing functions and the Gompertz model are presented in the appendix. Due to parameter unidentifiability $\lambda' = p\lambda$ is presented.

Site	Parameter	With forcing					Autonomous (no forcing)				
		Estimate	L 95% CL	U 95% CL	Z	P-value	Estimate	L 95% CL	U 95% CL	Z	P-value
Thailand	\hat{s}	0.317	0.294	0.341	3.9281	8.56e-05*	0.409	0.384	0.435	5.4355	7.58e-07*
	$\hat{\lambda}'$	1.71	1.60	1.83	4.2445	2.19e-05*	1.38	1.27	1.49	3.1356	0.0001198*
	$\hat{\theta}$	0.505	0.476	0.533	5.1048	3.31e-07*	0.576	0.542	0.610	6.2232	7.79e-08*
	$\hat{\alpha}$	2.25	2.07	2.41	2.2806	0.02257*	–	–	–	–	–
	\hat{T}_c	34.03	33.88	34.18	65.6596	<1e-15*	–	–	–	–	–
	$\hat{\sigma}_{\text{envs}}^2$	0.181					0.195				
Puerto Rico	\hat{s}	0.443	0.330	0.545	5.7289	1.01e-08*	0.395	0.217	0.591	4.1492	3.34e-05*
	$\hat{\lambda}'$	1.34	1.09	1.66	5.5511	2.84e-08*	1.23	0.61	2.07	3.3282	0.000874*
	$\hat{\theta}$	0.497	0.277	0.626	4.6662	3.07e-06*	0.539	0.256	0.825	3.9134	9.34e-05*
	$\hat{\alpha}$	–0.0213	–0.0257	–0.0121	–9.7436	<1e-15*	–	–	–	–	–
	$\hat{\beta}$	–0.161	–0.163	–0.158	–471.078	<1e-15*	–	–	–	–	–
	$\hat{\sigma}_{\text{envs}}^2$	0.303					0.364				

*Statistically significant ($P < 0.05$).

L, lower; U, upper; CL, confidence limits.

mental factors that are proportionally more uncertain around the median condition. In both Puerto Rico and Thailand, large sharp changes in mosquito population density can be explained by the impacts of forcing on the population dynamics (Fig. 3c and d), which seems to be reinforced by the nonstationary patterns of association between mosquito abundance and low kurtosis climatic factors: rainfall in Puerto Rico (Fig. S2a) and maximum temperature in Thailand (Fig. S2g). Models more successfully fitted the Thai data (Fig. S4b and d) than the Puerto Rico data (Fig. S4a and c). The importance of the forcing to explain abrupt changes in mosquito density is also reflected by model success to reproduce the original data. Fit of models considering the forcing (Fig. S4c and d) outperformed models without forcing (Fig. S4a and b). In fact, the role played by the forcing in shaping large nonmonotonic changes in mosquito density can be further observed in Fig. S5, which shows how simulations captured extreme mosquito densities when forcing was explicitly considered with nonlinear functions in both Puerto Rico (Fig. S5c) and Thailand (Fig. S5d), in contrast to when the forcing was ignored (Fig. S5a and b). Parameter estimates for the model presented in equation [1] indicated that dynamics at the nontrivial equilibrium are significantly ($P < 0.05$) stable in both Puerto Rico (Fig. S6a and c) and Thailand (Fig. S6b and d), a result confirmed by the mathematical analysis of the model (Appendix). A perturbation analysis of the best models with and without

forcing indicated that dynamics were most sensitive, in absolute terms, to changes in the parameter θ (Fig. 4a and b), and in relative terms to changes in λ' (Fig. 4c and d). Finally, we performed a reactivity analysis to gain insights into life history patterns that could transiently amplify the impacts of climatic forcing, or any other disturbance, on *Ae. aegypti* population dynamics. The reactivity analysis supplements our lack of data on larval dynamics, especially because immature survival, p , is encompassed in λ' , a key parameter in the dynamics as uncovered by the perturbation analysis. As parameters p and λ are nonidentifiable and only their product ($\lambda' = p\lambda$) can be estimated, we studied reactivity for combinations of λ' and p . It is important to note that unlike stability, in which these two parameters are multiplied to compute the dominant eigenvalue and determine the stability of a system, reactivity (i.e., the largest singular value of a model jacobian evaluated at equilibrium) is a function of these two parameters separately (see Appendix for details). We studied reactivity for combinations of p and λ that result in a value of λ' contained within the 95% confidence limits of the estimated parameters. In both Puerto Rico (Fig. 5a and c) and Thailand (Fig. 5b and d) low values of p , which imply large values of λ , lead to reactive dynamics, whereas large values of p (low λ) lead to nonreactive dynamics. The explicit consideration of the forcing increases the region of the parameter space where the model is nonreactive in Thailand, whereas for Puerto

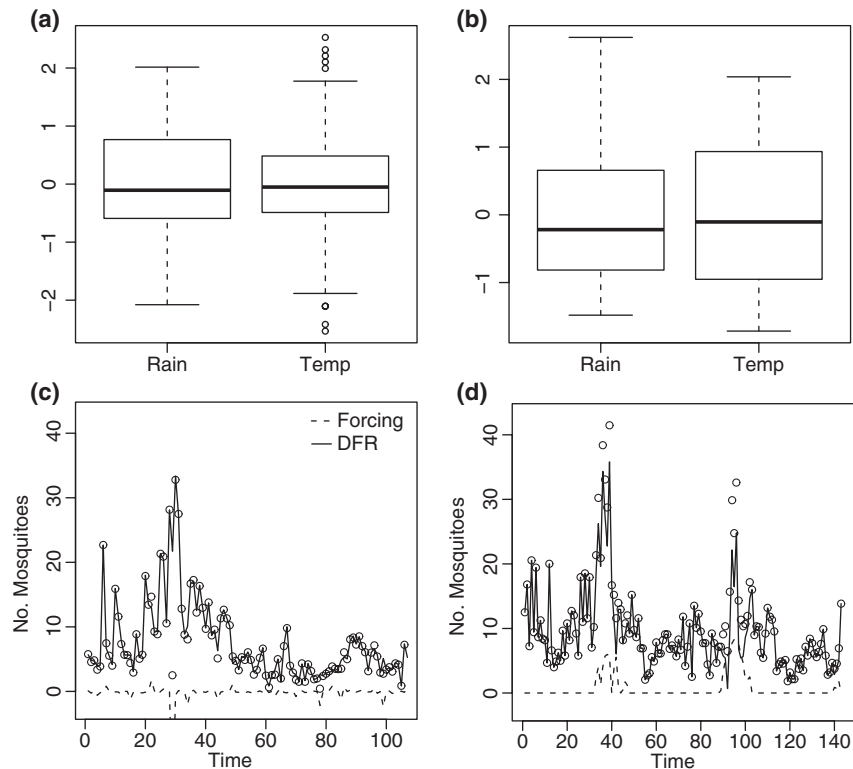


Fig. 3 Climatic variability and the impact of forcing on population dynamics. Boxplots for the standardized rainfall anomalies [Rain] and temperature range [Temp] of Puerto Rico (a) and Thailand (b), boxplot lines indicate quartiles and the median. Response to the forcing in Puerto Rico (c) and Thailand (d), dashed lines (Forcing in the legend) represent the changes in population density that can be attributed to the forcing, solid lines (DFR in the legend) represent population density after the forcing was subtracted and open circles represent the observed weekly abundance. For Puerto Rico, the kurtosis of rainfall anomalies was 2.53, and temperature range was 3.40. For Thailand, the kurtosis of rainfall anomalies was 2.80, and temperature range was 1.57. It is worth noticing that in both studies, sites outbreaks are linked to extreme events in the more platykurtic variables.

Rico they are similar. This point is better illustrated by the cross-section of the λ' estimates presented in Table 1 as function of p for Puerto Rico (Fig. 5e) and Thailand (Fig. 5f). In the former, there are no major differences between the reactivity of the forced and autonomous models, whereas in the latter, the forced model becomes reactive after reaching values of p smaller than those that trigger reactivity in the model without forcing.

Discussion

A major research theme in ecology is understanding population regulation, the tendency of populations to have bounded abundances (Royama, 1992; Turchin, 2003). In most cases, this observation is further supported by the ubiquity of stability in nonlinear population models when evaluated with parameters estimated from real populations (Hassell *et al.*, 1976; Ellner & Turchin, 1995; Kendall *et al.*, 1998). In fact, nonlinear population models have shown intrinsically

generated cycles and chaotic dynamics only in very few instances, with best examples coming from laboratory populations (Costantino *et al.*, 1997; Massie *et al.*, 2010). Although it is widely accepted that fluctuations around what seem to be stable regimes are due to environmental fluctuations (Sibly *et al.*, 2005, 2007; Ziebarth *et al.*, 2010), understanding forcing by environmental covariates is an elusive goal, which at best has been limited to the: (1) addition of linear functions (Chaves & Pascual, 2007; Yang *et al.*, 2008b), (2) description of nonstationary association patterns with different aspects of climate (Cazelles *et al.*, 2008; Chaves & Kitron, 2011), and (3) prediction of species phenology in seasonal environments (Taylor, 1981; Atkinson, 1994).

Herein, we exploit the detailed understanding of the life cycle and life history patterns of one of the best studied animal species, *Ae. aegypti* (Christophers, 1960; Dye, 1984; Legros *et al.*, 2009) using unique long-term abundance datasets from two very different regions of the world. From this analysis, we are able to gain

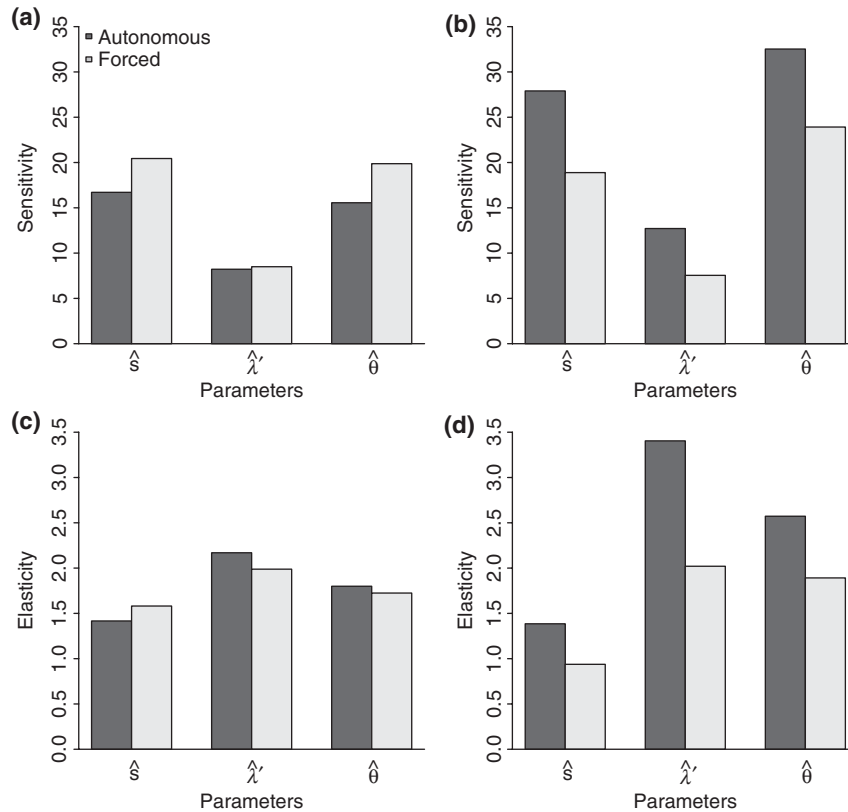


Fig. 4 Perturbation analysis for parameter estimates of the Gompertz Model. Results for Puerto Rico are presented in (a, c) and for Thailand in (b, d). (a and b) show sensitivity values at the nontrivial equilibrium. (c and d) show elasticity values at the nontrivial equilibrium. Dark gray bars indicate values for estimates from the autonomous models [i.e., models with no forcing] and light gray for the forced models [i.e., with climatic covariates].

insights into patterns of sensitivity of this species to changing environments that may be generalized to other species. Fluctuations in *Ae. aegypti* population density seem to be more sensitive to changes in factors whose pattern of variability is less bounded (lower kurtosis), or where normal conditions are more unstable over time. The relatively larger variability around the median in platykurtic distributions reflect patterns of variability that are very uncertain around the median conditions, e.g., circadian or seasonal cycles in the environment, or any regular change (Stearns, 1981), to which organisms can become adapted (Gause, 1942; Beissinger & Gibbs, 1993). Adaptation of individuals to more regular changes in the environment can generate a trade-off in their tolerance to other environmental factors (Schmalhausen, 1949; Gabriel *et al.*, 2005). Thus, in Thailand, the need to be adapted for a dry season is costly to mosquitoes, in the sense that fitness is probably reduced because larval habitats are water storage containers where crowding, i.e., high densities, can occur (Scott *et al.*, 2000; Schneider *et al.*, 2004). This, in turn, may

increase mosquito sensitivity to small changes in maximum temperature. Under crowding, it has been described that *Ae. aegypti* larvae are smaller and more sensitive to changes in the abundance of resources (Wada, 1965), and larval mortality increases at extreme temperatures (Bar-Zeev, 1958a). Following a massive mortality event in the larval population, triggered by high temperatures, population growth rate will increase and mosquito abundance can be expected to peak in subsequent weeks in an explosive, or over-compensatory way, as expected in a reactive population returning to its stable equilibrium. The lag of 10 weeks probably reflects that population build-up spans a few mosquito generations. This biologic mechanism also explains the nonstationary association with maximum temperature depicted by the wavelet analysis, which can increase mortality at high temperatures (Bar-Zeev, 1958a; Bar-Zeev, 1958b). In contrast, in Puerto Rico, the practical absence of a dry season releases mosquitoes from the need to colonize stable habitats, and the potential cost of intra-specific interactions is replaced by one of dynamic habitats associ-

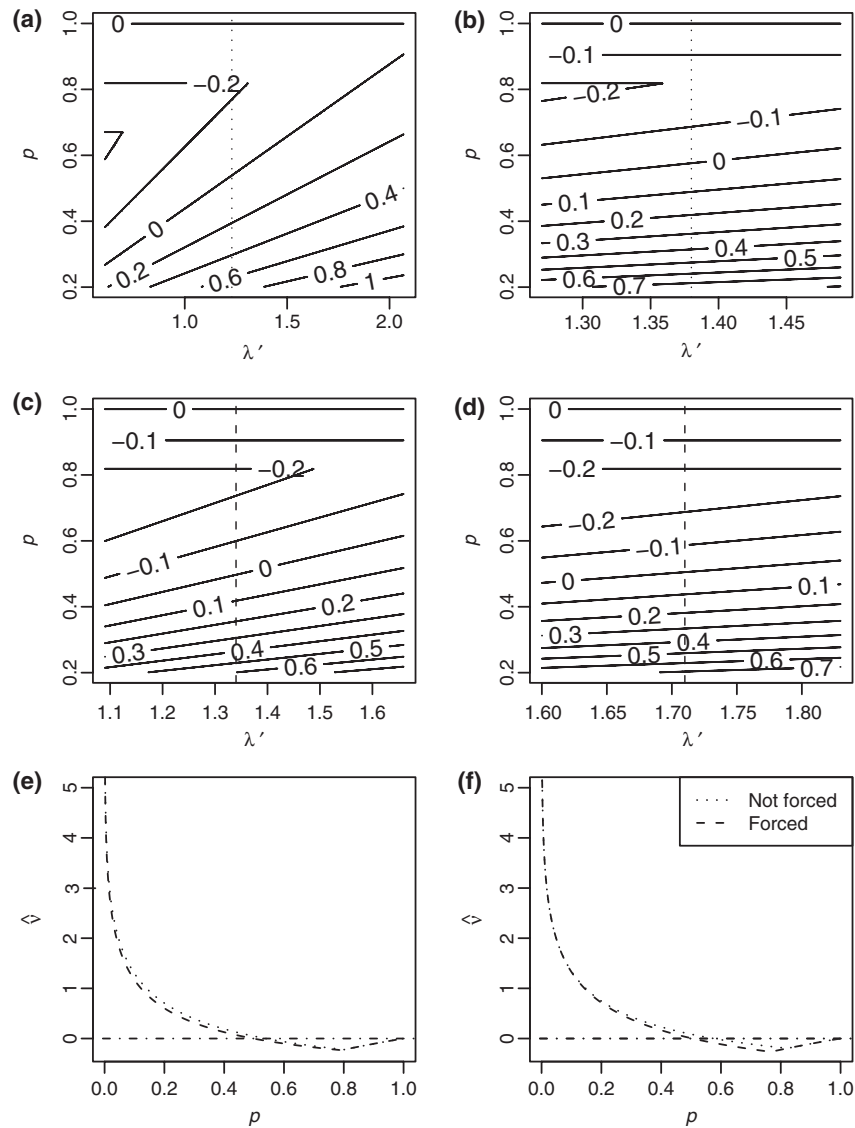


Fig. 5 Reactivity for the Gompertz model as function of the parameters p (juvenile survival) and λ (fecundity). Reactivity surfaces were constructed for the 95% confidence limits of the parameter $\hat{\lambda}'$ (x-axis, where $\hat{\lambda}' = p\lambda$) and values of p between 0.2 and 1 (y-axis). Contour lines indicate the values of reactivity (\hat{v}) for the different combinations of p and λ , for a given $\hat{\lambda}'$, from the autonomous Gompertz models of Puerto Rico (a) and Thailand (b) and the best forced models of Puerto Rico (c) and Thailand (d). Cross sections of the reactivity surface at the $\hat{\lambda}'$ estimates for the best autonomous and forced models of Puerto Rico (e) and Thailand (f). In the panels, $\hat{\lambda}'$ estimates (see Table 1) for the autonomous and forced models are indicated by dotted lines and dashed lines, respectively.

ated with rainfall. For example, in Puerto Rico, a large decrease in mosquito density at the beginning of the observations reflects the fact that *Ae. aegypti* females oviposit their eggs just above the water line in larval habitats (i.e., containers) and egg hatching is triggered by submersion in water or the high humidity that can be associated with rainfall (Reiter, 2007). Thus, a sequence of rainfall followed by lack of rainfall can drive sharp decreases in mosquito populations as observed in Puerto Rico.

This pattern, where populations present an increased sensitivity to small changes in factors other than those where their tolerance limits are constantly challenged was first described by Schmalhausen (1949). Schmalhausen's law asserts increased sensitivity by organisms to environmental factors that go beyond their normal variability when stressed by the fluctuations along their tolerance limits in any other dimension of existence (Chaves & Koenraad, 2010). Schmalhausen's law may be a guiding biologic principle that can be used to pre-

dict the most likely factors that explain climatic forcing in population dynamics, or the differences in patterns of association between environmental forces and abundance for the same species across different ecosystems. This principle is of major relevance in light of association between climate and vector-borne diseases, one of the major problems affecting humans and other organisms worldwide. In this sense, limitations of this study open venues for new research questions. Our focus on a relatively short span of climatic variability leads to questions on whether mosquito population responses are equal in abnormal years, such as those when El Niño Southern Oscillation modifies weather patterns in a way that generates climatic signatures on Dengue transmission dynamics (Thai *et al.*, 2010). More generally, whether population responses to forcing are context-dependent in light of seasonality. For example, the increased sensitivity to extreme temperatures in Thailand can be related to the existence of a dry and wet season, something not observed in Puerto Rico.

Although climatic variability seems to underlie sharp changes in the population density of *Ae. aegypti* in both sites density dependence can be described with functions of similar shape. The concave slope of the recruitment function, implied by $\hat{\theta}$, can explain the quick recovery of the populations (Sibly *et al.*, 2005) and the transient duration of population outbreaks. This is a pattern common to mosquito species elsewhere (Yang *et al.*, 2008a). Another noteworthy result is reactivity independent of climatic forcing. From a biologic perspective, it is important to notice that reactivity could reflect life-history trade-offs in mosquitoes. Although our model was limited in the sense that we could not estimate fecundity (λ) and larval survival (p) separately, the possibility that these parameters could be constrained to a fixed value (Stearns, 2000) implies that both parameters could trade-off and that large λ and low p lead to a reactive behavior as part of the life history strategy of *Ae. aegypti*. In both Thailand and Puerto Rico, the region of reactivity is slightly reduced when the forcing is considered explicitly, the population could be reactive to small perturbations in various combinations of juvenile survival and adult fecundity. These results are important in light of apocalyptic predictions about the impacts of climate change on vector-borne diseases based on models that do not reflect the biology of vectors and that do not use data to validate findings (Rogers & Randolph, 2000). The populations we studied are so tightly regulated that predictions of linear impacts of global warming on the abundance of mosquitoes, and the pathogens they transmit, such as those claiming that mosquito abundance and disease incidence will increase everywhere with warming temperatures, do not reflect mosquito

population dynamics, nor that dynamics can be influenced by vector control programs (Gubler, 1989; Wilson *et al.*, 1990). However, as demonstrated by this study (which is validated by high-quality data), dynamics of *Ae. aegypti* populations outbreaks are strongly linked to extraordinary climatic events, highlighting the need for further studies on the relationship between insect vectors of disease and climatic variability to make more accurate predictions about the impacts of climate change on insect vector population dynamics.

Detailed studies on insect vector and pest population dynamics in changing environments will similarly increase understanding of evolutionary changes that these populations may undergo in face of warming trends. Whether increases in climatic trends or variability change the ecological response of ectothermic organisms to changing environments is an overarching question in evolutionary ecology. Phenotypic plasticity could evolve in different directions depending on the tolerance to environmental gradients (Gabriel *et al.*, 2005). Changes in plasticity can modify traits that impact population dynamics and the ecosystem function of organisms (Gause, 1942; Schmalhausen, 1949; Levins, 1968; Gabriel *et al.*, 2005). For example, the canalization of environmental variability in *Ae. aegypti* body size is relevant to both vector competence for dengue virus (Schneider *et al.*, 2007) and to mosquito fitness (Bar-Zeev, 1957). In-depth research and analysis of organism-environment interactions is a pre-requisite for evidence-based decision and policy-making related to surveillance and suppression of vector-borne diseases in light of climate change.

Acknowledgements

Valuable comments were provided by Prof Chepina Hernandez, Prof N. Minakawa, Prof T. Takada, Dr A. Ponlawat, and Dr T. Revilla. LFC was supported by a Gorgas Memorial Research Award from the American Society of Tropical Medicine and Hygiene (ASTMH), and by a Grant in Aid for Research of Japan Society for the Promotion of Science (JSPS). UDK was supported by Emory University. UDK and TWS were supported by Research and Policy for Infectious Disease Dynamics (RAPIDD) mosquito-borne disease program of the Science and Technology Directorate and the Fogarty International Center, National Institutes of Health.

References

- Atkinson D (1994) Temperature and organism size – a biological law for ectotherms? *Advances in Ecological Research*, **25**, 1–58.
- Barbosa P, Peters TM, Greenough NC (1972) Overcrowding of mosquito populations: responses of larval *Aedes aegypti* to stress. *Environmental Entomology*, **1**, 89–93.
- Bar-Zeev M (1957) The effect of density on the larvae of a mosquito and its influence on fecundity. *Bulletin of Research Council of Israel B*, **6**, 220–228.
- Bar-Zeev M (1958a) The effect of extreme temperatures on different stages of *Aedes aegypti* (L.). *Bulletin of Entomological Research*, **48**, 593–599.

- Bar-Zeev M (1958b) The effect of temperature on the growth rate and survival of the immature stages of *Aedes aegypti* (L.). *Bulletin of Entomological Research*, **49**, 157–163.
- Beissinger SR, Gibbs JP (1993) Are variable environments stochastic? A review of methods to quantify environmental predictability. In: *Adaptation in Stochastic Environments* (eds Yoshimura J, Clark CW), pp. 132–146. Springer-Verlag, Berlin.
- Bolker BM (2008) *Ecological Models and Data in R*. Princeton University Press, Princeton.
- Caswell H (2008) Perturbation analysis of nonlinear matrix population models. *Demographic Research*, **18**, 59–115.
- Cazelles B, Chavez M, de Magny GC, Guegan JF, Hales S (2007) Time-dependent spectral analysis of epidemiological time-series with wavelets. *Journal of the Royal Society Interface*, **4**, 625–636.
- Cazelles B, Chavez M, Berteaux D, Menard F, Vik JO, Jenouvrier S, Stenseth NC (2008) Wavelet analysis of ecological time series. *Oecologia*, **156**, 287–304.
- Chaves LF, Koenraadt CJM (2010) Climate change and highland malaria: fresh air for a hot debate. *The Quarterly Review of Biology*, **85**, 27–55.
- Chaves LF, Pascual M (2006) Climate cycles and forecasts of cutaneous leishmaniasis, a nonstationary vector-borne disease. *Plos Medicine*, **3**, 1320–1328.
- Chaves LF, Pascual M (2007) Comparing models for early warning systems of neglected tropical diseases. *PLoS Neglected Tropical Disease*, **1**, e33.
- Chaves LF, Kitron UD (2011) Weather variability impacts on oviposition dynamics of the southern house mosquito at intermediate time scales. *Bulletin of Entomological Research*, **101**, doi: 10.1017/S0007485310000519.
- Christophers SR (1960) *Aedes aegypti* (L.) *The yellow fever mosquito: Its life history, bionomics and structure*. Cambridge University Press, Cambridge, 739 pp.
- Costantino RF, Desharnais RA, Cushing JM, Dennis B (1997) Chaotic dynamics in an insect population. *Science*, **275**, 389–391.
- Dye C (1982) Intraspecific competition amongst larval *Aedes aegypti* – food exploitation or chemical interference. *Ecological Entomology*, **7**, 39–46.
- Dye C (1984) Models for the population dynamics of the yellow fever mosquito, *Aedes aegypti*. *Journal of Animal Ecology*, **53**, 247–268.
- Edman JD (1988) Disease control through manipulation of vector-host interaction: some historical and evolutionary perspectives. In: *Proceedings of a Symposium: The Role of vector-host interactions in disease transmission* (eds Scott TW, Grumstrup-Scott J), pp. 43–50. Entomological Society of America, Washington, D.C.
- Ellner S, Turchin P (1995) Chaos in a noisy world: new methods and evidence from time series analysis. *American Naturalist*, **145**, 343–375.
- Focks DA, Haile DG, Daniels E, Mount GA (1993) Dynamic Life Table Model for *Aedes aegypti* (Diptera, Culicidae) – Analysis of the Literature and Model Development. *Journal of Medical Entomology*, **30**, 1003–1017.
- Gabriel W, Luttbeg B, Sih A, Tollrian R (2005) Environmental tolerance, heterogeneity, and the evolution of reversible plastic responses. *American Naturalist*, **166**, 339–353.
- Gause GF (1942) The relation of adaptability to adaptation. *The Quarterly Review of Biology*, **17**, 99–114.
- Gilpin ME, McClelland GAH (1979) Systems-analysis of the yellow-fever mosquito *Aedes aegypti*. *Fortschritte Der Zoologie*, **25**, 355–388.
- Gubler DJ (1989) *Aedes aegypti* and *Aedes aegypti*-borne disease control in the 1990s: top down or bottom up. *American Journal of Tropical Medicine and Hygiene*, **40**, 571–578.
- Harrington LC, Edman JD, Scott TW (2001) Why do female *Aedes aegypti* (Diptera : Culicidae) feed preferentially and frequently on human blood? *Journal of Medical Entomology*, **38**, 411–422.
- Hassell MP, Lawton JH, May RM (1976) Patterns of dynamical behavior in single-species populations. *Journal of Animal Ecology*, **45**, 471–486.
- Headlee TJ (1940) The relative effects on insect metabolism of temperatures derived from constant and variable sources. *Journal of Economic Entomology*, **33**, 361–364.
- Kendall BE, Prendergast J, Bjornstad ON (1998) The macroecology of population dynamics: taxonomic and biogeographic patterns in population cycles. *Ecology Letters*, **1**, 160–164.
- Legros M, Lloyd AL, Huang YX, Gould F (2009) Density-dependent intraspecific competition in the larval stage of *Aedes aegypti* (Diptera: Culicidae): revisiting the current paradigm. *Journal of Medical Entomology*, **46**, 409–419.
- Levins R (1968) *Evolution in Changing Environments. Some theoretical explorations*. Princeton University Press, Princeton, 120 pp.
- Levins R, Wilson M (1980) Ecological theory and pest-management. *Annual Review of Entomology*, **25**, 287–308.
- Magori K, Legros M, Puente ME, Focks DA, Scott TW, Lloyd AL, Gould F (2009) Skeeter buster: a stochastic, spatially explicit modeling tool for studying *Aedes aegypti* population replacement and population suppression strategies. *PLoS Neglected Tropical Disease*, **3**, e508.
- Mangel M (2006) *The Theoretical Biologist's Toolbox: Quantitative Methods for Ecology and Evolutionary Biology*. Cambridge University Press, Cambridge, 375 pp.
- Mardia KV (1970) Measures of multivariate skewness and kurtosis with applications. *Biometrika*, **57**, 519–530.
- Massie TM, Blasius B, Weithoff G, Gaedke U, Fussmann GF (2010) Cycles, phase synchronization, and entrainment in single-species phytoplankton populations. *Proceedings of the National Academy of Sciences*, **107**, 4236–4241.
- Neubert MG, Caswell H, Solow AR (2009) Detecting reactivity. *Ecology*, **90**, 2683–2688.
- Paaajmans KP, Blanford S, Bell AS, Blanford JJ, Read AF, Thomas MB (2010) Influence of climate on malaria transmission depends on daily temperature variation. *Proceedings of the National Academy of Sciences of the United States of America*, **107**, 15135–15139.
- Pascual M, Ahumada JA, Chaves LF, Rodo X, Bouma M (2006) Malaria resurgence in the East African highlands: temperature trends revisited. *Proceedings of the National Academy of Sciences of the United States of America*, **103**, 5829–5834.
- Pascual M, Cazelles B, Bouma MJ, Chaves LF, Koelle K (2008) Shifting patterns: malaria dynamics and rainfall variability in an African highland. *Proceedings of the Royal Society B-Biological Sciences*, **275**, 123–132.
- Ratikainen II, Gill JA, Gunnarsson TG, Sutherland WJ, Kokko H (2008) When density dependence is not instantaneous: theoretical developments and management implications. *Ecology Letters*, **11**, 184–198.
- Reiter P (2007) Oviposition, dispersal, and survival in *Aedes aegypti*: implications for the efficacy of control strategies. *Vector-Borne and Zoonotic Diseases*, **7**, 261–273.
- Rogers DJ, Randolph SE (2000) The global spread of malaria in a future, warmer world. *Science*, **289**, 1763–1766.
- Royama T (1992) *Analytical Population Dynamics*. Chapman and Hall, London.
- Schmalhausen II. (1949) *Factors of Evolution; The Theory Of Stabilizing Selection*. Blakiston Co., Philadelphia.
- Schneider JR, Morrison AC, Astete H, Scott TW, Wilson ML (2004) Adult size and distribution of *Aedes aegypti* (Diptera : Culicidae) associated with larval habitats in Iquitos, Peru. *Journal of Medical Entomology*, **41**, 634–642.
- Schneider JR, Mori A, Romero-Severson J, Chadee DD, Severson DW (2007) Investigations of dengue-2 susceptibility and body size among *Aedes aegypti* populations. *Medical and Veterinary Entomology*, **21**, 370–376.
- Scott TW, Morrison AC, Lorenz LH, et al. (2000) Longitudinal studies of *Aedes aegypti* (Diptera : Culicidae) in Thailand and Puerto Rico: population dynamics. *Journal of Medical Entomology*, **37**, 77–88.
- Shumway RH, Stoffer DS (2000) *Time Series Analysis And Its Applications*. Springer, New York, 572 pp.
- Sibly RM, Barker D, Denham MC, Hone J, Pagel M (2005) On the regulation of populations of mammals, birds, fish, and insects. *Science*, **309**, 607–610.
- Sibly RM, Barker D, Hone J, Pagel M (2007) On the stability of populations of mammals, birds, fish and insects. *Ecology Letters*, **10**, 970–976.
- Stearns SC (1981) On measuring fluctuating environments – predictability, constancy, and contingency. *Ecology*, **62**, 185–199.
- Stearns SC (2000) Life history evolution: successes, limitations, and prospects. *Naturwissenschaften*, **87**, 476–486.
- Stenseth NC, Mysterud A, Ottersen G, Hurrell JW, Chan K-S, Lima M (2002) Ecological effects of climate fluctuations. *Science*, **297**, 1292–1296.
- Taylor F (1981) Ecology and evolution of physiological time in insects. *American Naturalist*, **117**, 1–23.
- Thai KTD, Cazelles B, Nguyen NV et al. (2010) Dengue dynamics in Binh Thuan province, southern Vietnam: periodicity, synchronicity and climate variability. *PLoS Neglected Tropical Disease*, **4**, e747.
- Turchin P (2003) *Complex Population Dynamics*. Princeton University Press, Princeton.
- Wada Y (1965) Effect of larval density on the development of *Aedes aegypti* (L.) and the size of adults. *Quaestiones entomologicae*, **1**, 223–249.
- Wilson ML, Agudelo-Silva F, Spielman A (1990) Increased abundance, size, and longevity of food-deprived mosquito populations exposed to a fungal larvicide. *American Journal of Tropical Medicine and Hygiene*, **43**, 551–556.
- Yang G-J, Bradshaw C, Whelan P, Brook B (2008a) Importance of endogenous feedback controlling the long-term abundance of tropical mosquito species. *Population Ecology*, **50**, 293–305.
- Yang G-J, Brook BW, Whelan PI, Cleland S, Bradshaw CJA (2008b) Endogenous and exogenous factors controlling temporal abundance patterns of tropical mosquitoes. *Ecological Applications*, **18**, 2028–2040.
- Ziebarth NL, Abbott KC, Ives AR (2010) Weak population regulation in ecological time series. *Ecology Letters*, **13**, 21–31.

Supporting Information

Additional Supporting Information may be found in the online version of this article:

Appendix S1. Detailed methods.

Table S1. Model selection. Study site indicates the study site (Puerto Rico or Thailand), Model indicates the density-dependence model (Beverton-Holt, Gompertz or Ricker), Stochasticity indicates whether the model had Observation or Environmental stochasticity, Form indicates whether covariates were considered linearly (Linear) or nonlinearly (Threshold, etc.), $-\loglik$ is the negative log-likelihood of the model, Parameters is the number of parameters considered by the model, AIC is the Akaike Information criterion for the models, BIC the Bayes information criterion for the model, and ΔAIC & ΔBIC the difference with respect to the minimum value.

Figure S1. Seasonality of the studied periods and background seasonality. Rainfall in (a) Puerto Rico, (b) Thailand, Temperature range in (c) Puerto Rico, (d) Thailand. Boxplots represent the seasonal distribution of climatic variables (estimated with data from 1951 to 2011). Blue and red lines represent the records from our study periods for rainfall and temperature range, respectively. For the estimates, we used freely available monthly data from the US National Oceanic and Atmospheric Administration, NOAA (<ftp://ftp.ncdc.noaa.gov/pub/data/ghcn/v2/>) for San Juan, Puerto Rico (Station 435785260), and for Thailand, we used data from Bangkok (Station 228484550, the closest location to Chachoengsao with long climatic records). For Thailand, it is worth noticing that temperature data from 1972 to 1995 were missing, the time period including the study period at Chachoengsao (1990–1993). In general, climatic patterns for our study periods were encompassed by the overall seasonal variability of the study sites. However, February & March 1993 in Puerto Rico, and March & April in 1992 in Thailand had an extreme temperature range when compared with their long-term seasonal profile.

Figure S2. Time domain descriptive analysis of mosquito density N_t . Autocorrelation Function, ACF, for Puerto Rico (a) and Thailand (c); Partial Autocorrelation Function, PACF, for Puerto Rico (b) and Thailand (d); Cross correlation functions between N_t and: rainfall in Puerto Rico (e) and Thailand (g) Average temperature in Puerto Rico (f) and Thailand (h); maximum temperature in Puerto Rico (i) and Thailand (k), and minimum temperature in Puerto Rico (j) and Thailand (l). Blue dashed lines indicate 95% confidence intervals of correlation expected by random, i.e., peaks outside the band indicate a significant correlation. The x -axis indicates time lags (in weeks) and the y -axis are correlation values [i.e., contained in $(-1,1)$].

Figure S3. Time frequency domain descriptive analysis. Cross-wavelet coherency and phase of mosquito abundance in Puerto Rico with (a) rainfall, (b) average temperature, (c) maximum temperature, and (d) minimum temperature; and in Thailand with (e) rainfall, (f) average temperature, (g) maximum temperature, and (h) minimum temperature. In each panel, the top plot shows coherency and the bottom plot shows the phase. The coherency scale is from zero (blue) to one (red). Red regions in the upper part of the plots indicate frequencies and times for which the two series share variability. The cone of influence (within which results are not influenced by the edges of the data) and the significant ($P < 0.05$) coherent time–frequency regions are indicated by solid lines. The colors in the phase plots correspond to different lags between the variability in the two series for a given time and frequency, measured in angles from $-\pi$ to π . A value of π corresponds to a lag of 26 weeks. A smoothing window of 26 weeks ($2w + 1 = 53$) was used to compute the cross-wavelet coherence.

Figure S4. Model fitting, fitted \hat{N}_t vs observed N_t mosquito densities for the best autonomous models for Puerto Rico (a) and Thailand (b) and the best forced models for Puerto Rico (c) and Thailand (d). \hat{r} indicates the estimated Pearson correlation between \hat{N}_t and N_t for the model presented in each panel.

Figure S5. Model Simulation. Summary of 1000 simulations for the best autonomous models for Puerto Rico (a) and Thailand (b), and the best forced models for Puerto Rico (c) and Thailand (d). For all the iterations (a.k.a., time steps) of each model, we computed the 95% confidence limits (blue lines) and the median (green lines) of the simulations. Red lines represent sample simulations. Open circles represent the population density (i.e., observed data) in panels for autonomous models (i.e., a and b) and the population density with the forcing subtracted (DFR in Fig. 3 of the main text) in panels for forced models (i.e., c and d). In the forced models, we show DFR, because for the simulations, we excluded the impact of the forcing. For the simulations, we employed parameter estimates from Table 1 and equation (1) from the main text to generate realizations of the best autonomous and forced models. We used as initial conditions, the first and second observations of the observed time series for the Puerto Rico models (107 realizations per simulation) and observations nine and 10 of the observed time series for the Thailand models (143 realizations per simulation). This figure shows that, in general, simulations of the autonomous models were unable to capture the most extreme values of the observed data.

Figure S6. Bootstrap of the stability. Parametric bootstraps to test the stability of the Gompertz model with parameter estimates for the best autonomous (i.e., no forcing) models of (a) Puerto Rico, (b) Thailand, and the best forced models of (c) Puerto Rico and (d) Thailand. Plots present the distribution of the largest eigenvalues (ξ) from the jacobian of 10 000 simulations of the corresponding Gompertz model assuming neutral stability (i.e., the distribution is expected to have a mean of 1). The y -axis is the probability density for a given value of ξ , i.e., the x -axis. The dashed lines represent the estimated dominant eigenvalues $\hat{\xi}$ of the jacobian evaluated at the nontrivial equilibrium using parameter estimates of the best models presented in Table 1. In all four cases, the null hypothesis that stability is neutral (i.e., not different from 1) is rejected ($P < 0.05$, P -values for the specific models are presented in each panel), as $\hat{\xi}$ is significantly smaller than 1 in each case. These results indicate that models are stable, because the largest eigenvalue for each model is contained within the unit circle, the stability criterion for discrete time models (Levins & Wilson, 1980).

Please note: Wiley-Blackwell are not responsible for the content or functionality of any supporting materials supplied by the authors. Any queries (other than missing material) should be directed to the corresponding author for the article.

Appendix: Detailed Methods

Descriptive Time Series Analysis

We examined the correlation structure of the mosquito time series by using standard techniques for time series analysis. These included the **autocorrelation function, ACF**, which is the correlation of the elements in a time series through several time lags. The **partial autocorrelation function, PACF**, which considers the correlation between consecutive time lags (not the whole time series like the **ACF**) and the **Cross correlation function, CCF**, which presents the correlation between two time series across time lags (Shumway *et al.*, 2000). To compute the **CCF**, we used the pre-whitened residuals (Chaves, 2009) of the climatic time series (rainfall and mean, minimum, maximum temperature) and the residuals of a second order autoregressive model, **AR(2)**, fitted to each mosquito time series. The pre-whitening consists of filtering the climatic time series with the estimated coefficients of the AR(2) model fitted to the mosquito abundance time series. This process ensures that correlations are not spurious results of similar autocorrelation structures in the two time series (Chaves, 2009). All these preliminary analyses are in the time domain, which for the cross-correlation analysis assumes that associations are constant over time. However, associations between time series can be very localized in time, producing a non-stationary (i.e., non-constant) association through time (Cazelles *et al.*, 2007). Thus, we also studied the association between the climatic time series and the mosquito abundance series using **cross-wavelet analysis** (Cazelles *et al.*, 2007). This analysis allowed us to determine how the association between the two time series changed over time at different periods (i.e., non-stationarity). The **cross-wavelet coherency analysis** shows the frequencies at which the two times series have high power, an indicator of concerted fluctuations, and the **cross-wavelet phase analysis** shows the time lag separating the association between the two series. For further technical details of cross-wavelet analysis, see Cazelles *et al.* (2007)

Models

Delayed Ricker Model

This model assumes that adult mosquito population (N_t) is described by the following equation:

$$N_t = \lambda N_{t-1} \exp(-b N_{t-2}) \quad (1)$$

The delayed Ricker model comes from the integration, assuming a constant per capita growth rate for a discrete time interval (Turchin, 2003), of the delayed logistic equation (Hutchinson, 1948):

$$\frac{dN(t)}{dt} = rN(t) \left(1 - \frac{N(t-\tau)}{K}\right) \quad (2)$$

where K is the carrying capacity of a population, r the per-capita growth rate and τ is the time delay in which density impact population growth. Therefore the parameter λ represents the population growth rate in discrete time ($\exp(r)$) and b is the inverse of K .

Delayed Beverton-Holt and Gompertz Models

We can consider that individuals in an adult mosquito population (N_t) at time t come from the surviving adults (N_{t-1}) and the recruitment from emerging juvenile individuals (J_{t-1}) in the previous time step, $t-1$, as described by the function $H(N,J)$:

$$N_t = H(N_{t-1}, J_{t-1}) \quad (3)$$

$$N_t = sN_{t-1} + p J_{t-1}$$

Where s is the per-capita survival rate of adults and p is the per-capita emerging probability of juveniles. Equation (3) assumes that juveniles either emerge as adults, with probability p , or die, with probability $1-p$, after one time step. For weekly data this is an appropriate assumption, the pre-imaginal developmental time of *Aedes aegypti* averages a week (Headlee, 1940, Headlee, 1941, Bar-Zeev, 1958b) under the temperatures experienced in Puerto Rico and Thailand. Experiments and observations suggest that the density-dependence regulation of *Aedes aegypti* (Legros *et al.*, 2009, Dye, 1984, Gilpin *et al.*, 1979) occurs primarily during the immature stages. Assuming that density-dependence can be represented by a function $G(N)$ that describes the regulatory processes acting upon the production of juveniles (i.e., larvae and eggs), we have:

$$J_t = G(N_{t-1}) \quad (4)$$

In *Aedes aegypti* larval density does not seem to affect adult emergence success when resources are unlimited (Dye, 1982, Wada, 1965, Barbosa *et al.*, 1972, Bar-Zeev, 1957). However, emerging individuals are shorter and less fecund (Briegel *et al.*, 2002, Bar-Zeev, 1957). Thus, if we assume that fecundity decreases with adult density, when larval mortality is constant, a carrying capacity ($1/b$) emerges which can be represented by a Beverton-Holt function (Turchin, 2003):

$$J_t = \frac{\lambda N_{t-1}}{1 + b N_{t-1}} \quad (5)$$

Where λ can have a similar interpretation as in equation (2) or alternatively can be seen as a per capita fecundity. Alternatively, the carrying capacity ($1/b$) can emerge if the mortality of immatures increases with adult density under a constant fecundity, or if both fecundity and mortality are density-dependent. Equation 3 can be written as function of adults mosquitoes in any stage by substituting equation 5:

$$N_t = sN_{t-1} + p \left(\frac{\lambda N_{t-2}}{1 + b N_{t-2}} \right) \quad (6)$$

For the Gompertz model (Sibly *et al.*, 2005) a phenomenological exponent θ , whose value is constrained in $(0,1)$, is used for the function $G(N)$ so that $J_t = \lambda N_{t-1}^\theta$, resulting in the following equation:

$$N_t = sN_{t-1} + p(\lambda N_{t-2}^\theta) \quad (7)$$

Stochasticity in the models

We made two assumptions about stochasticity in models (1), (6) and (7). First, we assumed that all models had an additive observation normal error (Bolker, 2008). Under this assumption observations (n_t), i.e., the left side of equations (1), (6) and (7) for each time step, t , are considered to be normal, i.e., $n_t \sim N(N_t, \sigma_{obs}^2)$. Second, we assumed the presence of environmental stochasticity, which is defined as perturbations affecting all individuals in a population at a given time (Mangel, 2006). Under this assumption, the left and right hand side of equations (1), (6) and (7) are log-transformed (Dennis *et al.*, 1994), and the resulting left hand side of the equation, z_t , is assumed to be normal, i.e., $z_t \sim N(\log(N_t), \sigma_{envs}^2)$.

Exogenous forcing in the models

Following results from the descriptive time series analysis, i.e., the cross-correlation and cross-wavelet analyses, it was clear that mosquito population dynamics were primarily influenced by rainfall in Puerto Rico and by maximum temperature in Thailand. In the case of Puerto Rico, Environmental Covariates (EC), included total rainfall (R) and the weekly difference in rainfall (ΔR), with a one week lag. We included the difference in rainfall because both habitat dynamics and egg hatching in *Aedes aegypti* are sensitive both to the quantity of water and its relative change, e.g., eggs hatch after flooded with water (Gilpin *et al.*, 1979, Christophers, 1960). For Thailand, EC s included maximum temperature with 10 (T_{t-10}) weeks of lag. Also since impacts of temperature in insects can be cumulative (Taylor, 1981, Taylor, 1982) we included the summation of average temperatures up to lag 10 (CT_{t-10}). To test if impacts of temperature were due to its variability, we also included measures of its cumulative variability by computing the first principal component from a matrix of lagged average temperatures, including the previous 10 (PCT_{t-10}) weeks. The first principal component was computed by applying the coefficients from the eigenvector associated with the dominant eigenvalue of the variance covariance matrix of the lagged temperatures.

To include the effects of the environmental forcing, we defined three different functions, $EXO()$, which were added to the stochastic versions of the three density-dependent models in equations (1, 6 & 7). The first function was a simple linear one:

$$EXO(EC_t) = \alpha EC_t \quad (8)$$

Where the coefficient α measures the impact of changes in the EC . The second function was a threshold function defined as:

$$EXO(EC_t) = \begin{cases} 0 & \text{if } EC_t < EC_c \\ \alpha(EC_t - EC_c) & \text{if } EC_t \geq EC_c \end{cases} \quad (9)$$

Where there is an environmental impact only when the EC exceeds a threshold value (EC_c) measured by the coefficient α . The third function was a saturating hyperbolic function, also known in ecology as a Holling Type II, where the impact of rainfall (or its difference) reaches a saturating level for high values:

$$EXO(EC_t) = \frac{\alpha EC_t}{1 + \beta EC_{t-1}} \quad (10)$$

In Puerto Rico, the three functions (8, 9 and 10) were used with $EC=R$ or $EC=\Delta R$. In Thailand, the function presented in (8) was used with $EC=T$ or $EC=CT$ or $EC=PCT$, and the function described in (9) with $EC=T$.

Although N_t was correlated with both average and maximum Temperature (Fig. S1H, S1K), we only show the results for maximum temperature because the likelihoods for most models were minimized with maximum temperature (including the best models), there was a clear threshold for the impact of temperature on the Thai N_t (Fig. 2D), the use of the threshold function was able to depict the nonstationary pattern of association between the Thai N_t and maximum Temperature (Fig. S2G and Fig. 3D) and there is a plausible biological mechanism for the observation: extreme temperatures increase the mortality of *Aedes aegypti* (Bar-Zeev, 1958a), which is known to at least alleviate density-dependence in this species (Wilson *et al.*, 1990, Wada, 1965).

Models considered the two possible pathways proposed by Stenseth *et al* (2002) to quantify the role of exogenous forcing on density-dependent population dynamics. First, the forcing is additive to the density-dependent dynamics (*DDM*):

$$N_t = DDM + EXO \quad (11)$$

Or the forcing can impact multiplicatively population density:

$$N_t = (DDM)(EXO) \quad (12)$$

Maximum Likelihood Estimation

Observation error

We assumed data with a normal distribution, $N(N_t | \alpha, \sigma_{obs}^2)$, whose likelihood (L_{N_t}) can be expressed as:

$$L_{N_t}(\alpha) = \prod_1^t f(n_t | \alpha) \quad (13)$$

Where N_t is a normal random variable whose observed mean (n_t) is determined by a vector of parameters α , σ_{obs}^2 is the variance of the random variable, t the length of the time series and f is the normal probability function. Then, the log-likelihood is:

$$\ln L_{N_t}(\alpha) = \sum_1^t \ln f(n_t | \alpha) \quad (14)$$

Given the non-linearity of the equations (1), (6) and (7) no exact solution for the maximization of the parameters likelihood can be found analytically and numerical approximations need to be used. Thus for parameter estimation of the model presented in (1) the variance is minimized by the following equation:

$$\hat{\sigma}_{obs}^2 = \frac{1}{t} \sum_1^t (n_t - \lambda n_{t-1} \exp(-bn_{t-2}))^2 \quad (15)$$

Given the multiplication of parameters in equations (6) and (7) $\lambda p = \lambda'$. Therefore for parameter estimation of equation (6) the following variance is minimized numerically:

$$\hat{\sigma}_{obs}^2 = \frac{1}{t} \sum_1^t \left(n_t - sn_{t-1} - \lambda' \left(\frac{n_{t-2}}{1+bn_{t-2}} \right) \right)^2 \quad (16)$$

And this expression for equation (7):

$$\hat{\sigma}_{obs}^2 = \frac{1}{t} \sum_1^t (n_t - sn_{t-1} - \lambda' n_{t-2}^\theta)^2 \quad (17)$$

When the exogenous forcing (*EXO*) was included in an additive manner, the following equation for the variance was minimized:

$$\hat{\sigma}_{obs}^2 = \frac{1}{t} \sum_1^t (n_t - DDM - EXO)^2 \quad (18)$$

Where *DDM* is the right hand side of equations for any of the three density –dependent models presented in (1), (6) and (7). When the exogenous forcing was considered in a multiplicative manner, the following equation for the variance was minimized:

$$\hat{\sigma}_{obs}^2 = \frac{1}{t} \sum_1^t (n_t - DDM * EXO)^2 \quad (19)$$

Environmental error

Here, we that assumed log transformed mosquito abundance, $z_t = \log(N_t)$, had a normal distribution, $N(z_t | \alpha, \sigma_{envs}^2)$, whose likelihood ($L_{\log(N_t)}$) can be expressed as follows:

$$L_{\log(N_t)}(\alpha) = \prod_1^t f(z_t | \alpha) \quad (20)$$

Where α , f and σ_{envs}^2 have a similar interpretation to the case of observation error (see equation 13), the only difference being that σ_{envs}^2 is environmental variability. Parameters for equations (1), (6) and (7) were obtained by minimizing the following equation:

$$\hat{\sigma}_{envs}^2 = \frac{1}{t} \sum_1^t (z_t - \log(DDM))^2 \quad (21)$$

DDM is the right hand side of each density–dependent model presented in (1), (6) and (7). To consider the forcing we assumed that it was additive:

$$\hat{\sigma}_{envs}^2 = \frac{1}{t} \sum_1^t (z_t - \log(DDM + EXO))^2 \quad (22)$$

And multiplicative:

$$\hat{\sigma}_{envs}^2 = \frac{1}{t} \sum_1^t (z_t - \log(DDM) - \log(EXO))^2 \quad (23)$$

Optimization

For the numerical optimization, we used a combined strategy, in which, initial parameter estimates were obtained by a global optimization using 1×10^8 iterations of simulated annealing, and the initial estimates were further optimized by using the Nelder-Mead algorithm until convergence. Parameter

estimation was performed with the open-access statistical language R using the stats, base and bbmle libraries (Bolker, 2008)

Likelihood for Model Selection

Log transformation of time series data render their log-likelihood smaller than that of untransformed data (Chaves, 2009). To make a sound comparison between observational and environmental noise models we back-transformed the likelihood of models with environmental variability. Since data was log-transformed, the sum of the log-transformed original time series needs to be added to the log-likelihood obtained with equations (21), (22) and (23). For further details see the appendix of Chaves (2009)

Stability and reactivity analysis of the model with the best fit

Stability analysis is performed to set the conditions that allow a population to persist or invade a habitat (Levins *et al.*, 1980). For both study sites the best model for density-dependence was the delayed Gompertz model (7). The model can also be seen as a two stage class model according to equations (3) and (4):

$$\begin{pmatrix} N_t \\ J_t \end{pmatrix} = \begin{pmatrix} s & p \\ \lambda(\cdot)^\theta & 0 \end{pmatrix} \begin{pmatrix} N_{t-1} \\ J_{t-1} \end{pmatrix} \quad (24)$$

Where $\mathbf{A} = \begin{pmatrix} s & p \\ \lambda(\cdot)^\theta & 0 \end{pmatrix}$ is the model transition matrix.

The stability of (24) was studied by first finding its equilibria. The model reaches an equilibrium (N^*, J^*) when there are no changes over time :

$$\begin{pmatrix} N^* \\ J^* \end{pmatrix} = \mathbf{A} \begin{pmatrix} N^* \\ J^* \end{pmatrix} \quad (25)$$

The trivial equilibrium is:

$$(N^*=0, J^*=0) \quad (26)$$

and the non-trivial equilibrium is:

$$\left(N^* = \left(\frac{p\lambda}{1-s} \right)^{1/(1-\theta)} ; J^* = \lambda \left(\frac{p\lambda}{1-s} \right)^{\theta/(1-\theta)} \right) \quad (27)$$

To examine the stability of the equilibria, we computed the jacobian (φ) of the system presented in (24):

$$\varphi = \begin{pmatrix} \frac{\partial H}{\partial N} & \frac{\partial H}{\partial J} \\ \frac{\partial G}{\partial N} & \frac{\partial G}{\partial J} \end{pmatrix} = \begin{pmatrix} s & p \\ \lambda\theta(N)^{\theta-1} & 0 \end{pmatrix} \quad (28)$$

Where $H(N,J)$ and $G(N)$ are functions defined in (3) and (4). We evaluated the jacobian at equilibrium (φ^*), that is when $N = N^*$, and determined the dominant eigenvalues from its characteristic equation $\det(\varphi^* - \xi I) = 0$:

$$\xi^2 - s\xi - p\lambda\theta N^{*(\theta-1)} = 0 \quad (29)$$

Which led to the following expression for the eigenvalues (ξ):

$$\xi = \frac{s}{2} \pm \sqrt{\left(\frac{s}{2}\right)^2 + \theta N^{*(\theta-1)}} \quad (30)$$

For the trivial equilibrium, (26), the system is always unstable since, given the constraint of θ to be within the open interval (0,1), $N^{*(\theta-1)}$ converges to values outside the unit circle, where a discrete time system of equations is unstable, i.e., $|\xi| > 1$ (Levins *et al.*, 1980). For the non-trivial equilibrium, equation (27), the dominant eigenvalue is:

$$\xi = \frac{s}{2} + \sqrt{\left(\frac{s}{2}\right)^2 + \theta(1-s)} \quad (31)$$

Where the system is stable, i.e., $|\xi| < 1$ (Levins *et al.*, 1980), as long as:

$$\sqrt{\left(\frac{s}{2}\right)^2 + \theta(1-s)} < 1 - \frac{s}{2} \quad (32)$$

Which after some algebra simplifies to the following relationship:

$$\theta < 1 \quad (33)$$

Which is always true, provided that $0 < \theta < 1$, i.e., that there is density-dependent regulation in the system. The condition for asymptotic stability of the model presented in (33) also implies that the system cannot undergo neither fold (a.k.a., tangent) nor flip (a.k.a., period doubling) bifurcations, as they will require a value of $\theta \geq 1$ (Kuznetsov, 2004). Neimark-Sacker bifurcation, the discrete time analog of the Hopf bifurcation, is also not possible for the parameter set of biological sound models, since survival is smaller or equal to one by definition, i.e., $s \leq 1$. This parameter constraint renders complex solutions to equation (31) impossible, a necessary condition of the Neimark-Sacker bifurcation (Kuznetsov, 2004).

Significance of the estimated stability ($\hat{\xi}$)

To test the significance of the estimated stability ($\hat{\xi}$), we performed **parametric bootstraps**. For $\hat{\xi}$ we assumed neutral-stability as the null hypothesis ($\hat{\xi} = 1$). The alternative hypotheses are instability ($\hat{\xi} > 1$) or asymptotic stability ($\hat{\xi} < 1$). A parametric distribution of ξ was generated by simulating equation (7) with environmental noise 10000 times. Then, we compared the estimated $\hat{\xi}$ to the distribution of ξ under the null hypothesis. To generate a parametric distribution of ξ we used the recipe presented by Neubert *et al* (2009) in which equation (28) is simulated in a way that produces 1 as the average largest

eigenvalue. We tested the significance of the stability for the model presented in (7) using parameter estimates obtained both with and without the consideration of the exogenous forcing for each study site.

Reactivity is the maximum instantaneous growth rate of a small perturbation to a system (Caswell *et al.*, 2005). It also can be used as an index of transient behavior in the sense that a positive value predicts a transient, i.e., quick, amplification of a perturbation around an equilibrium (Neubert *et al.*, 2009). To compute reactivity (v) we used the equation derived by Caswell and Neubert (2005) for discrete time systems:

$$v = \log \zeta(\varphi) \quad (34)$$

Where ζ is the largest singular value, a.k.a. spectral norm (Verdy *et al.*, 2008) of the jacobian matrix, φ , presented in equation (28). Equation (34) also has the bonus of being a general result that predicts the reactivity of a system even in the absence of a thorough sampling of initial perturbations (Caswell and Neubert, 2005), an advantage over tracking the amplification of perturbations of different size by repeated model iteration.

We pursued the reactivity analysis because it can provide insights on the role that stage structure can have on mosquito population outbreaks. The derivation of the best model, delayed Gompertz, as both a discrete time equation in (7) and a stage structured matrix in (24), shows that $\lambda' = \lambda p$. The emergence probability of immatures, p , is, by definition, constrained to the interval [0,1]. Thus, given a value of λ' and a value of p is possible to find a value for $\lambda = \frac{\lambda'}{p}$. This estimated λ can be imputed into equation (28) to compute the reactivity of the Gompertz model for combinations of λ' and p using equation (34).

Perturbation analysis

We studied the response of the model selected as best to changes in parameter values, a.k.a. **perturbation analysis**. We used the two most common metrics to measure the impacts of changes in parameters in population dynamics, sensitivity which measures the total change in a response function (e.g., the population size at equilibrium) to changes in a parameter, and elasticity which measures the proportional change in a response function to changes in a parameter (Caswell, 2008). To Compute the sensitivity we used the following equation derived by Caswell (2008):

$$\frac{dN^*}{d\omega^T} = \left(I_s - \mathbf{A} - (N^{*T} \otimes I_s) \frac{\partial \text{vec} \mathbf{A}}{\partial N^T} \right)^{-1} (N^{*T} \otimes I_s) \frac{\partial \text{vec} \mathbf{A}}{\partial \omega^T} \quad (35)$$

Where N^* is a 2x1 vector with the equilibrium for the adult population (N^*), ω is a vector of parameters $\omega = (s, \lambda', \theta)$, where $\lambda' = p\lambda$. \mathbf{A} is the projection matrix presented in equation (24). In the case of the model presented in (7) equation (35) reduces to:

$$\frac{dN^*}{d\omega^T} = \left(1 - s - \lambda' \theta (N^*)^{(\theta-1)} \right)^{-1} \begin{pmatrix} N^* & 0 & 0 \\ 0 & (N^*)^{(\theta)} & \lambda' \ln(N^*) (N^*)^{(\theta)} \end{pmatrix} \quad (36)$$

To compute the elasticity, e , of the equilibrium population, N^* , to changes in the parameter ω_i we used the following equation presented by Caswell (2008):

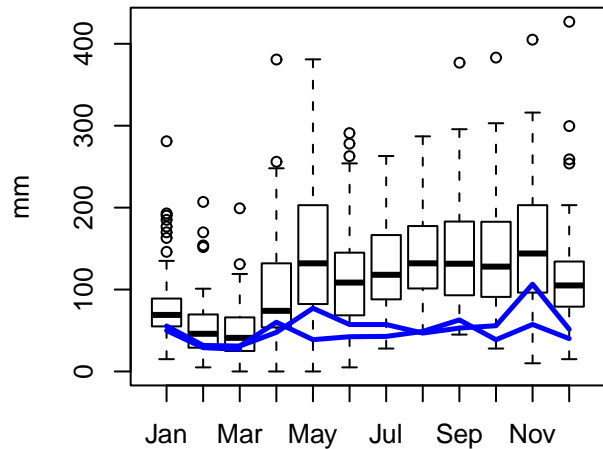
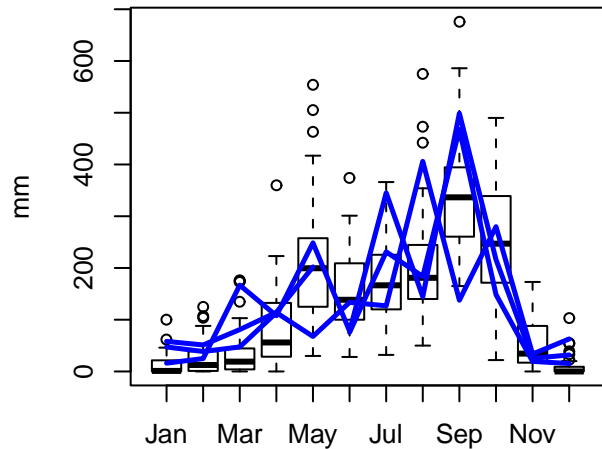
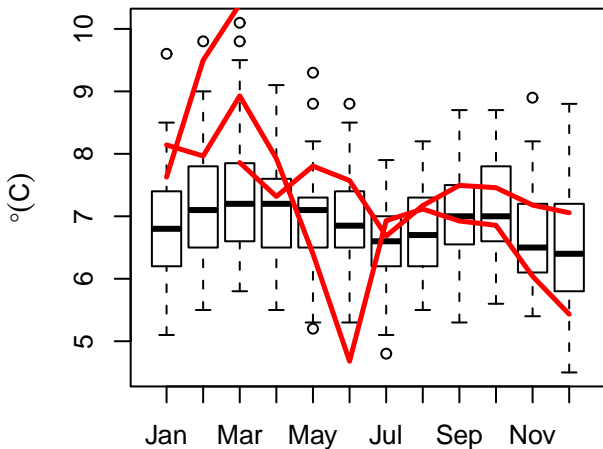
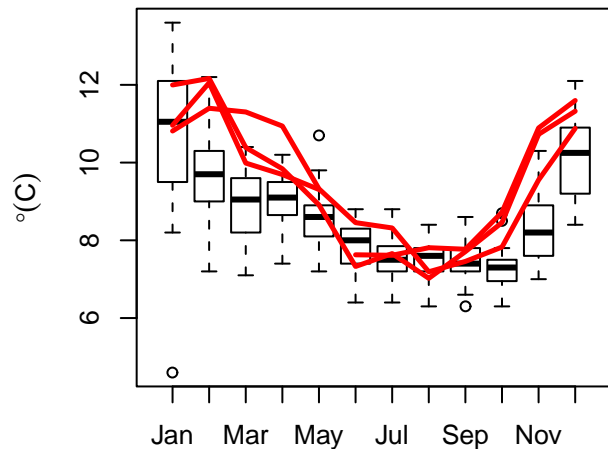
$$e_i = \frac{\omega_i}{N^*} \frac{dN^*}{d\omega_i} \quad (37)$$

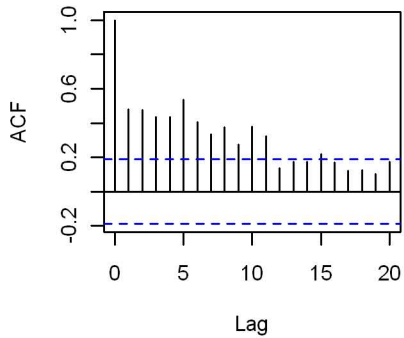
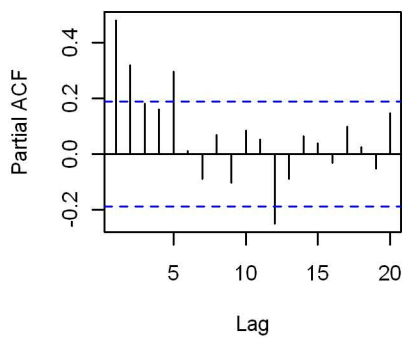
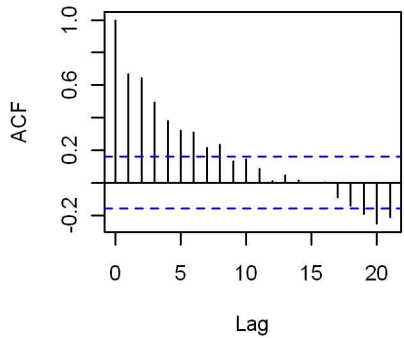
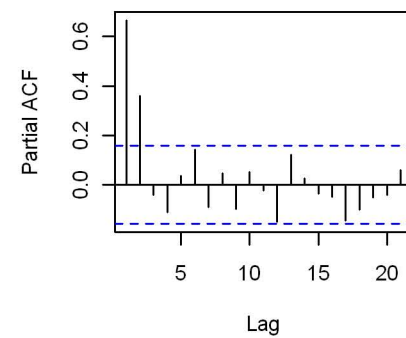
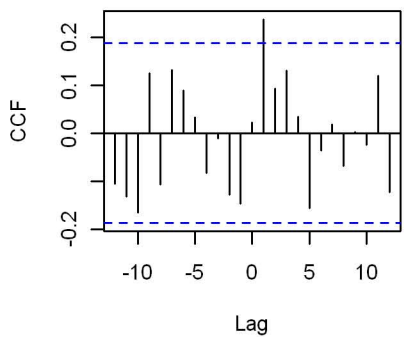
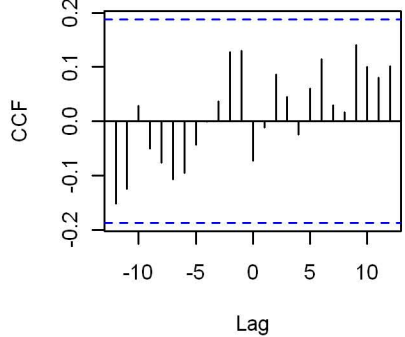
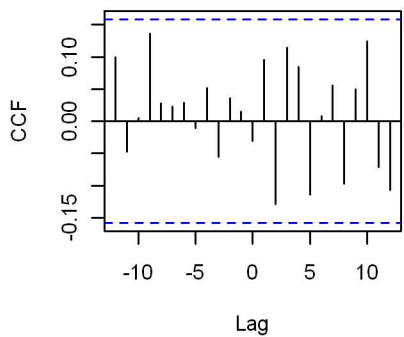
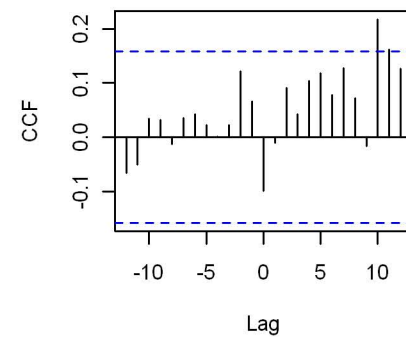
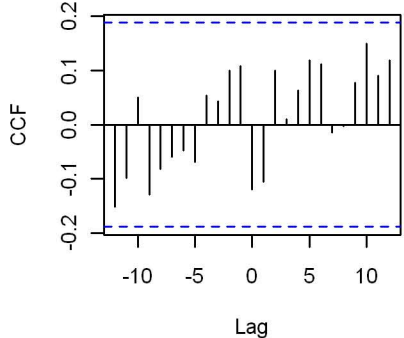
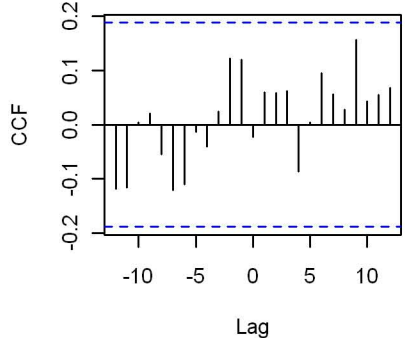
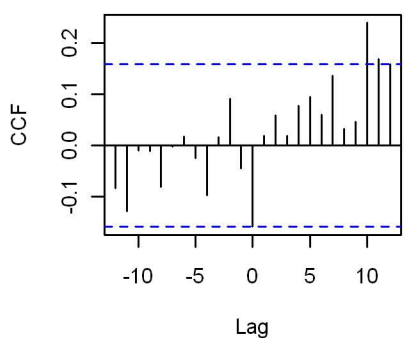
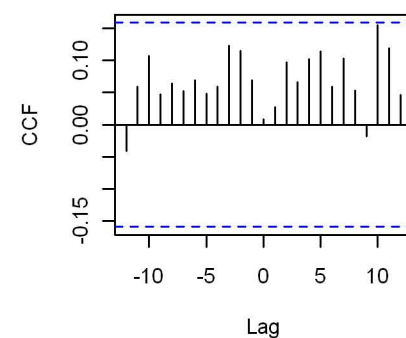
We computed the sensitivity and elasticity of the non-trivial equilibrium for the model presented in (7) with environmental noise, and using parameter estimates both with and without the consideration of the exogenous forcing for both study sites.

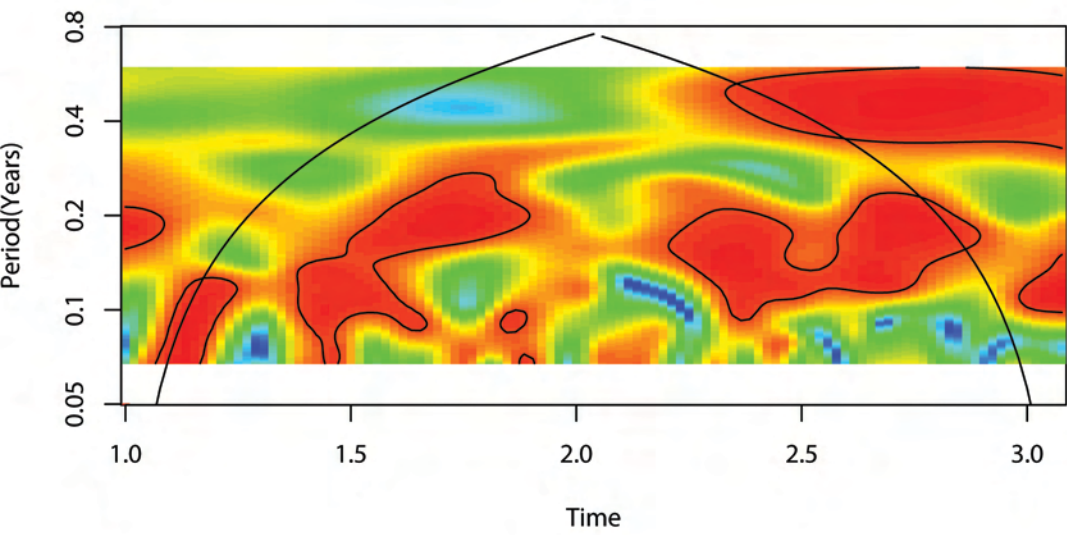
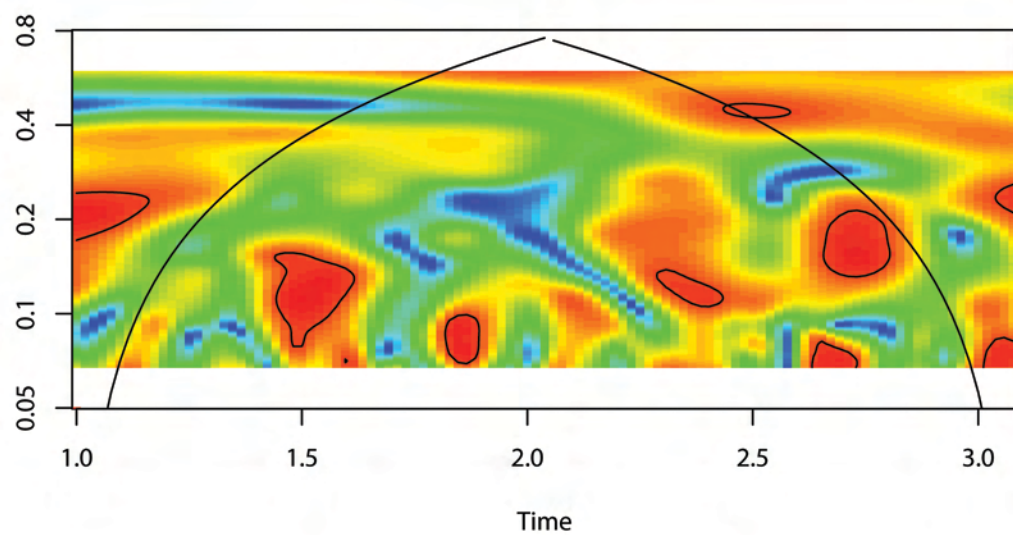
References

- Bar-Zeev M (1957) The effect of density on the larvae of a mosquito and its influence on fecundity. *Bull Res Counc of Israel B*, **6**, 220-228.
- Bar-Zeev M (1958a) The effect of extreme temperatures on different stages of *Aedes aegypti* (L.). *Bulletin of Entomological Research*, **48**, 593-599.
- Bar-Zeev M (1958b) The effect of temperature on the growth rate and survival of the immature stages of *Aedes aegypti* (L.). *Bulletin of Entomological Research*, **49**, 157-163.
- Barbosa P, Peters TM, Greenough NC (1972) Overcrowding of mosquito populations: Responses of larval *Aedes aegypti* to stress. *Environmental Entomology*, **1**, 89-93.
- Bolker BM (2008) *Ecological Models and Data in R*. Princeton University Press, Princeton
- Briegleb H, Hefti M, DiMarco E (2002) Lipid metabolism during sequential gonotrophic cycles in large and small female *Aedes aegypti*. *Journal of Insect Physiology*, **48**, 547-554.
- Caswell H (2008) Perturbation analysis of nonlinear matrix population models. *Demographic Research*, **18**, 59-115.
- Caswell H, Neubert MG (2005) Reactivity and transient dynamics of discrete-time ecological systems. *Journal of Difference Equations and Applications*, **11**, 295-310.
- Cazelles B, Chavez M, de Magny GC, Guegan JF, Hales S (2007) Time-dependent spectral analysis of epidemiological time-series with wavelets. *Journal of the Royal Society Interface*, **4**, 625-636.
- Chaves LF (2009) Climate and recruitment limitation of hosts: the dynamics of American cutaneous leishmaniasis seen through semi-mechanistic seasonal models. *Annals of Tropical Medicine and Parasitology*, **103**, 221-234.
- Christophers SR (1960) *Aedes aegypti* (L) *The yellow fever mosquito: Its life history, bionomics and structure*. Cambridge University Press, Cambridge, 739 pp.
- Dennis B, Taper ML (1994) Density Dependence in Time Series Observations of Natural Populations: Estimation and Testing. *Ecological Monographs*, **64**, 205-224.
- Dye C (1982) Intraspecific Competition Amongst Larval *Aedes aegypti* - Food Exploitation or Chemical Interference. *Ecological Entomology*, **7**, 39-46.
- Dye C (1984) Models for the Population Dynamics of the Yellow Fever Mosquito, *Aedes aegypti*. *Journal of Animal Ecology*, **53**, 247-268.
- Gilpin ME, McClelland GAH (1979) Systems-Analysis of the Yellow-Fever Mosquito *Aedes aegypti*. *Fortschritte Der Zoologie*, **25**, 355-388.
- Headlee TJ (1940) The Relative Effects on Insect Metabolism of Temperatures Derived from Constant and Variable Sources. *Journal of Economic Entomology*, **33**, 361-364.
- Headlee TJ (1941) Further studies of the relative effects on insect metabolism of temperatures derived from constant and variable sources. *Journal of Economic Entomology*, **34**, 171-174.
- Hutchinson GE (1948) Circular Causal Systems in Ecology. *Annals of the New York Academy of Sciences*, **50**, 221-246.

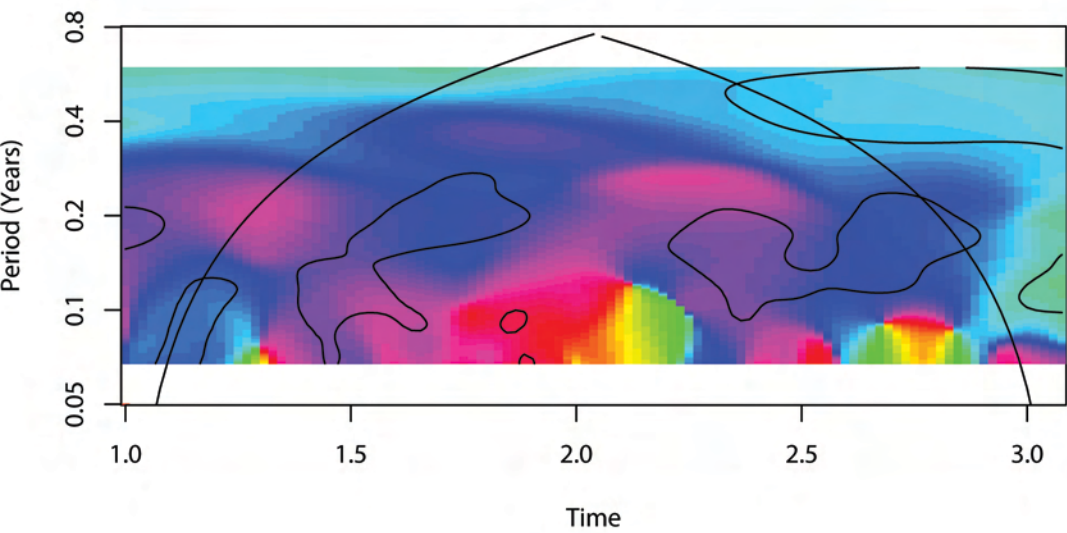
- Kuznetsov YA (2004) *Elements of applied bifurcation theory*. Springer, New York, 631 pp.
- Legros M, Lloyd AL, Huang YX, Gould F (2009) Density-Dependent Intraspecific Competition in the Larval Stage of *Aedes aegypti* (Diptera: Culicidae): Revisiting the Current Paradigm. *Journal of Medical Entomology*, **46**, 409-419.
- Levins R, Wilson M (1980) Ecological Theory and Pest-Management. *Annual Review of Entomology*, **25**, 287-308.
- Mangel M (2006) *The theoretical biologist's toolbox: quantitative methods for Ecology and Evolutionary Biology*. Cambridge University Press, Cambridge, 375 pp.
- Neubert MG, Caswell H, Solow AR (2009) Detecting reactivity. *Ecology*, **90**, 2683-2688.
- Shumway RH, Stoffer DS (2000) *Time series analysis and its applications*. New York: Springer, 572 pp.
- Sibly RM, Barker D, Denham MC, Hone J, Pagel M (2005) On the Regulation of Populations of Mammals, Birds, Fish, and Insects. *Science*, **309**, 607-610.
- Stenseth NC, Mysterud A, Ottersen G, Hurrell JW, Chan KS, Lima M (2002) Ecological effects of climate fluctuations. *Science*, **297**, 1292-1296.
- Taylor F (1981) Ecology and Evolution of Physiological Time in Insects. *American Naturalist*, **117**, 1-23.
- Taylor F (1982) Sensitivity of Physiological Time in Arthropods to Variation of Its Parameters. *Environmental Entomology*, **11**, 573-577.
- Turchin P (2003) *Complex population dynamics*. Princeton University Press, Princeton.
- Verdy A, Caswell H (2008) Sensitivity analysis of reactive ecological dynamics. *Bulletin of Mathematical Biology*, **70**, 1634-1659.
- Wada Y (1965) Effect of larval density on the development of *Aedes aegypti* (L.) and the size of adults. *Quaestiones entomologicae*, **1**, 223-249.
- Wilson ML, Agudelo-Silva F, Spielman A (1990) Increased Abundance, Size, and Longevity of Food-Deprived Mosquito Populations Exposed to a Fungal Larvicide. *American Journal of Tropical Medicine and Hygiene*, **43**, 551-556.

A**B****C****D**

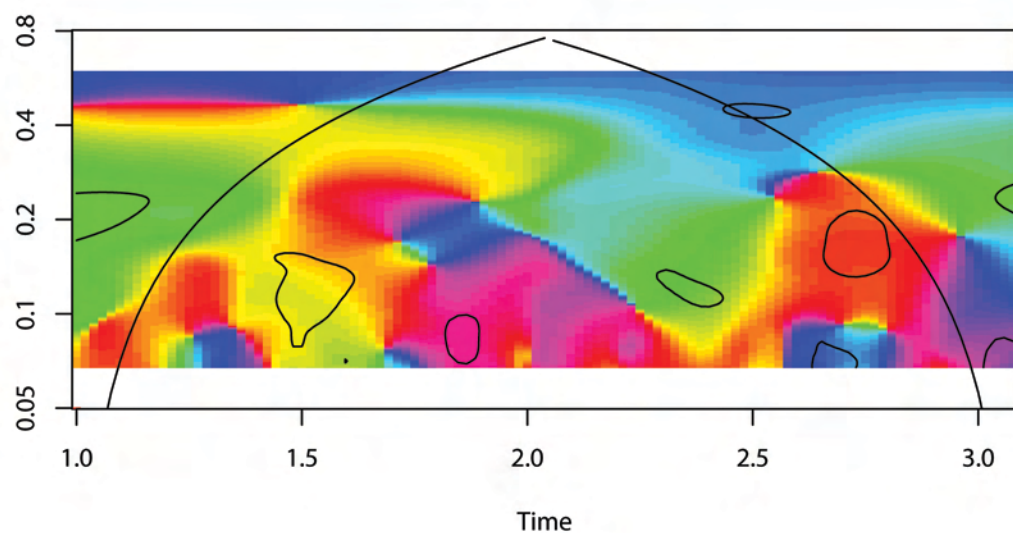
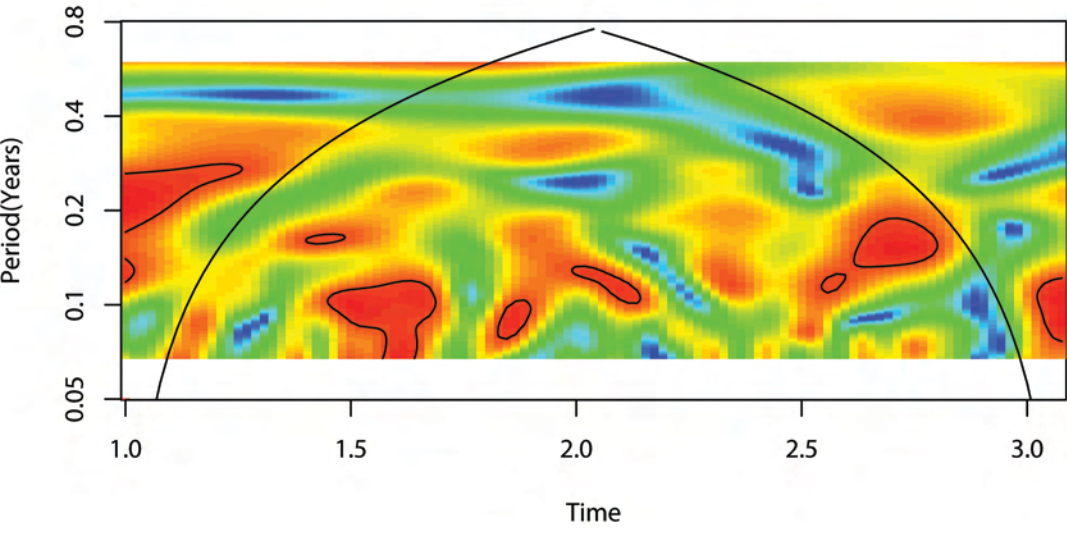
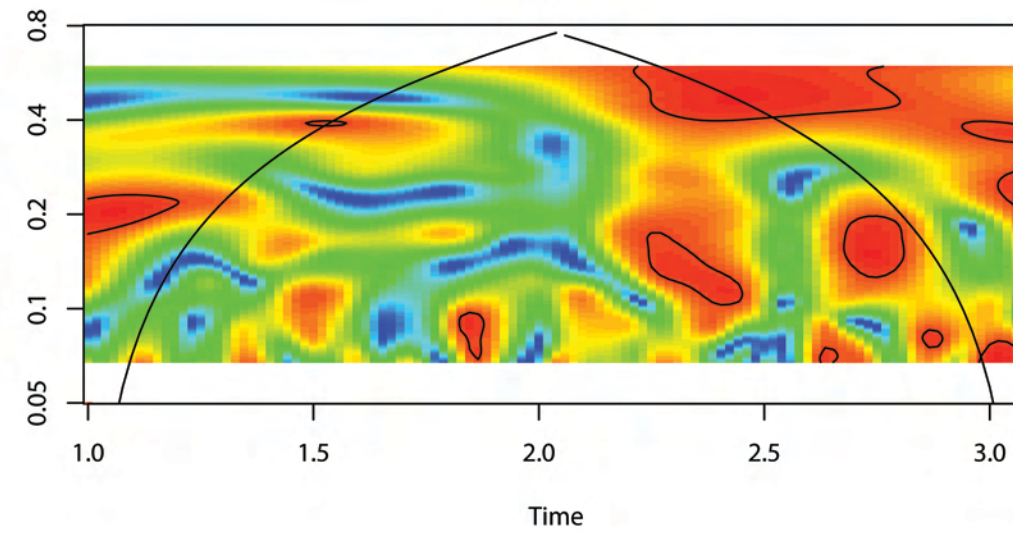
A**B****C****D****E****F****G****H****I****J****K****L**

A**B**

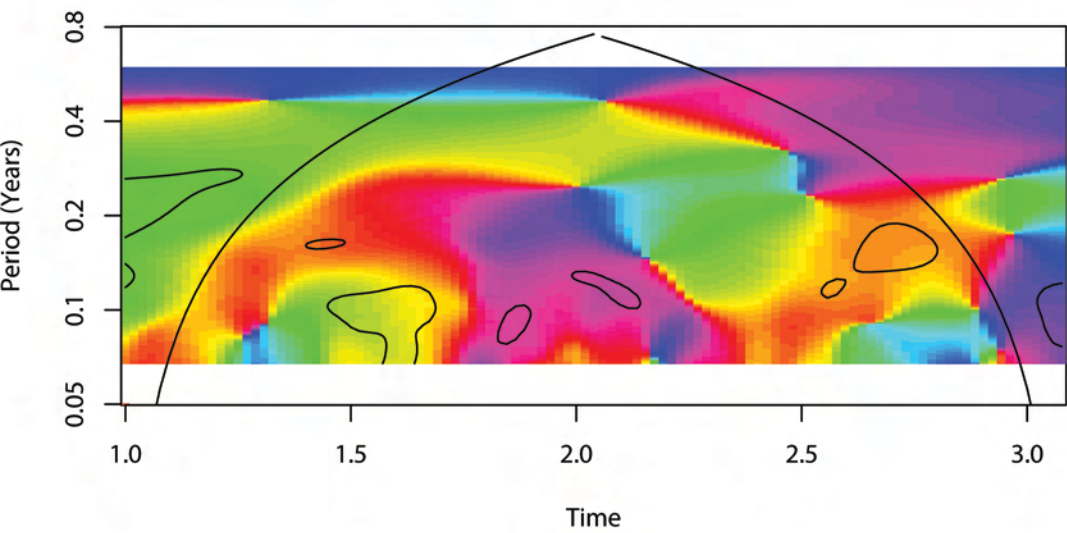
Phase



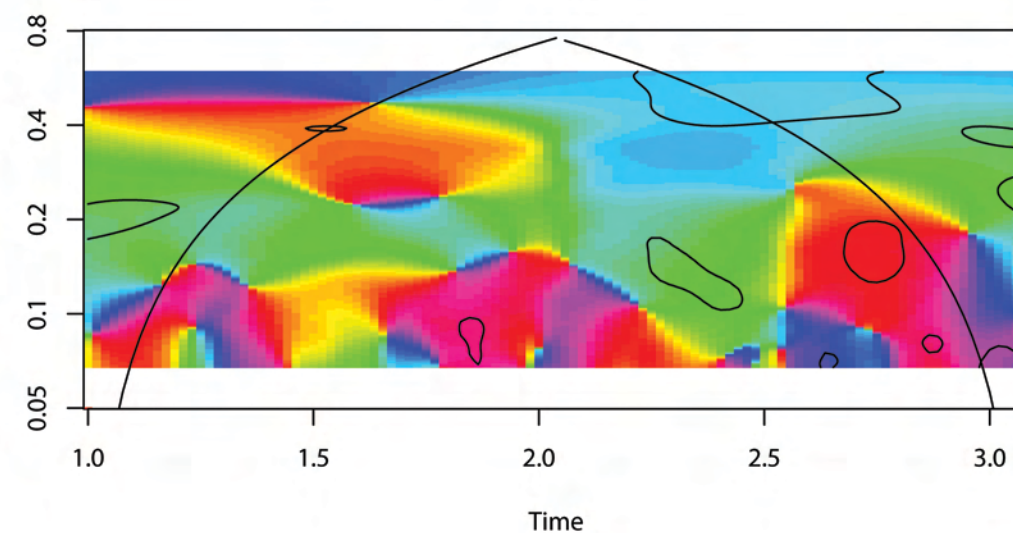
Phase

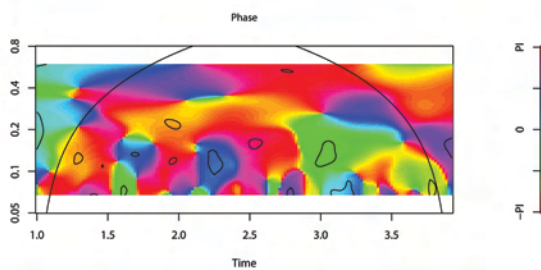
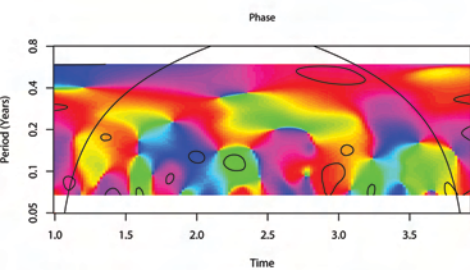
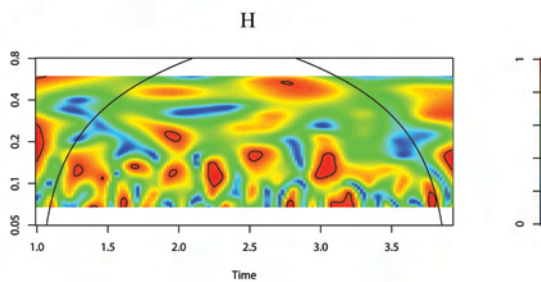
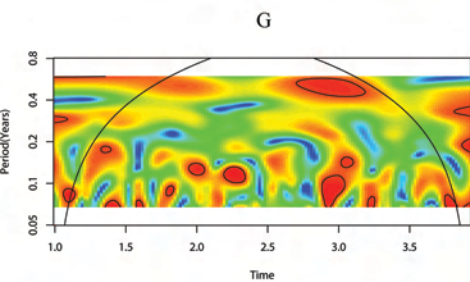
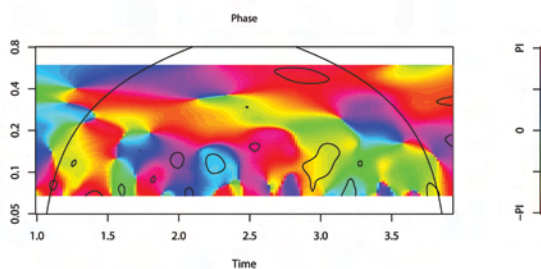
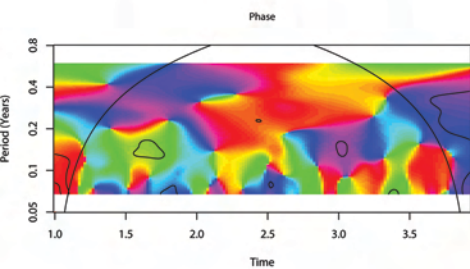
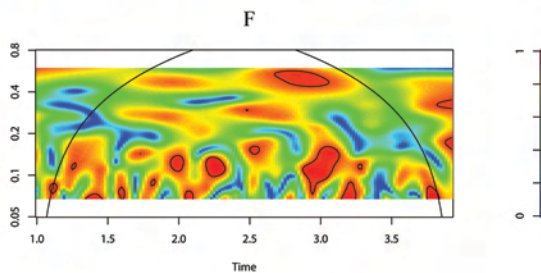
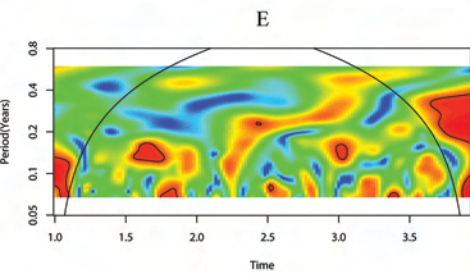
**C****D**

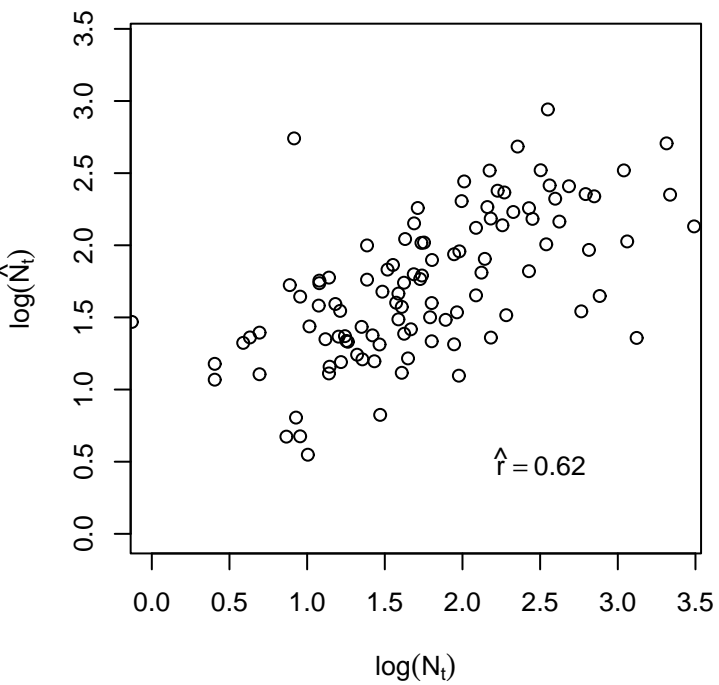
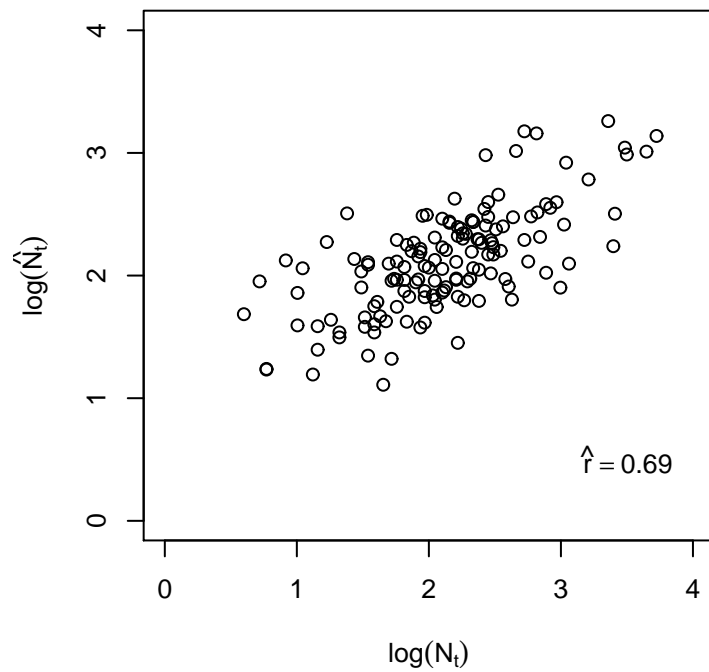
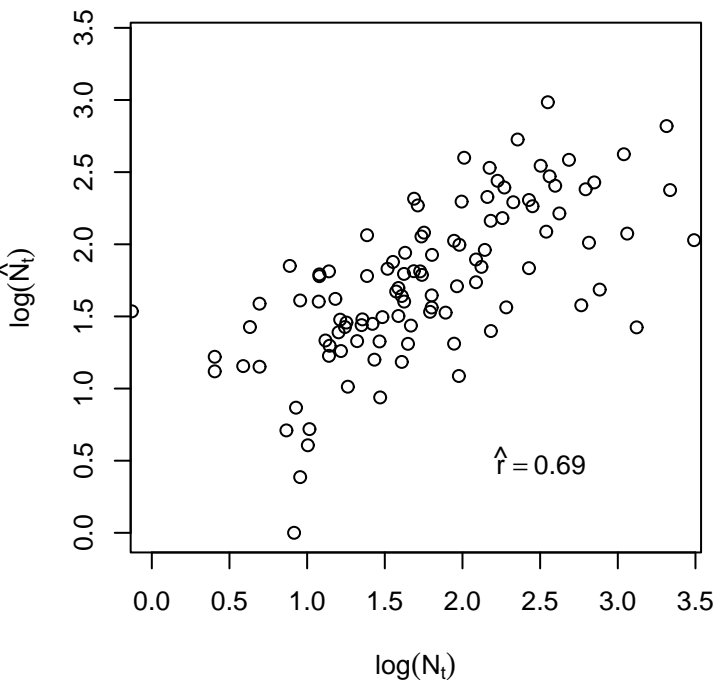
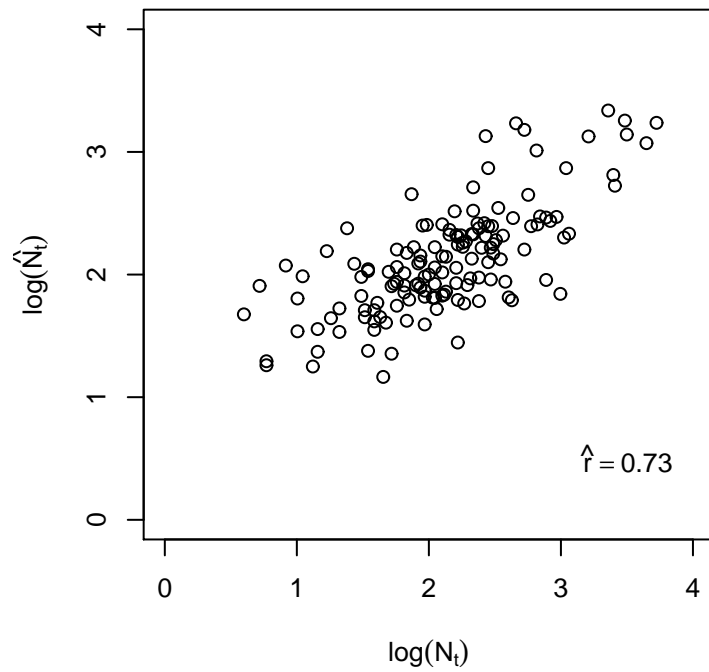
Phase

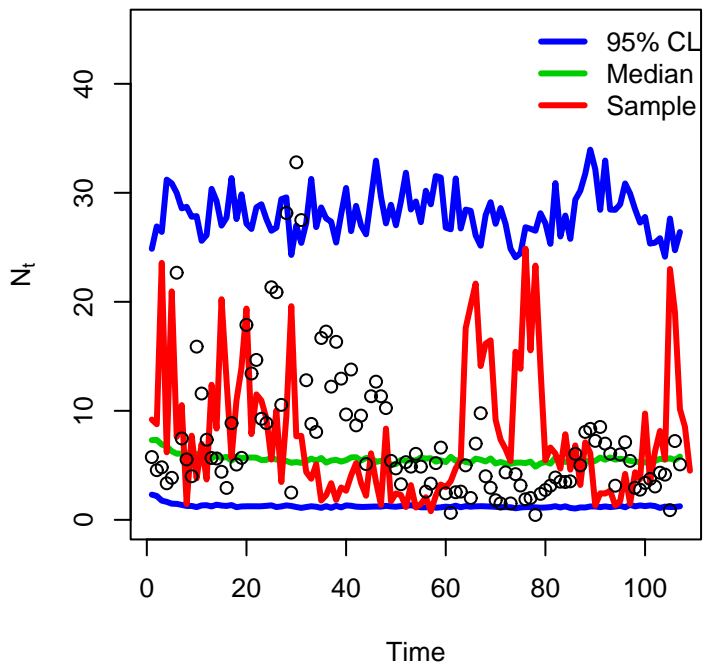
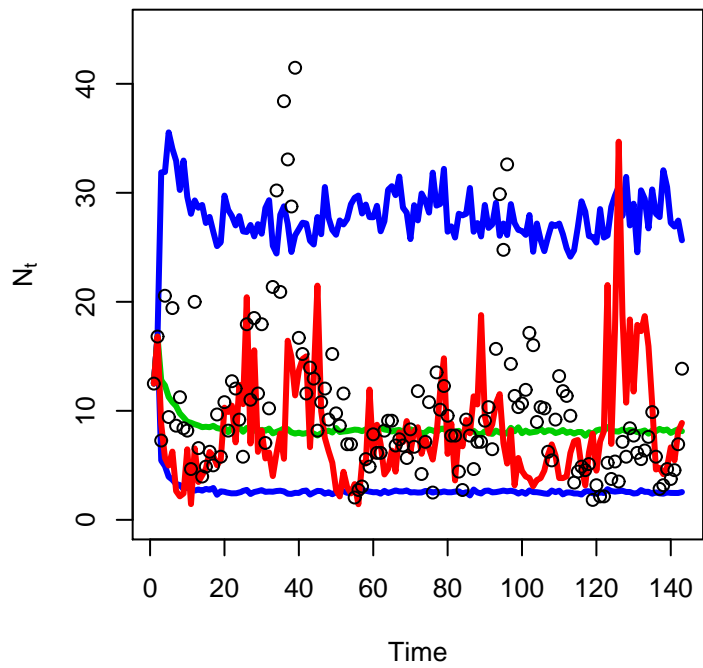
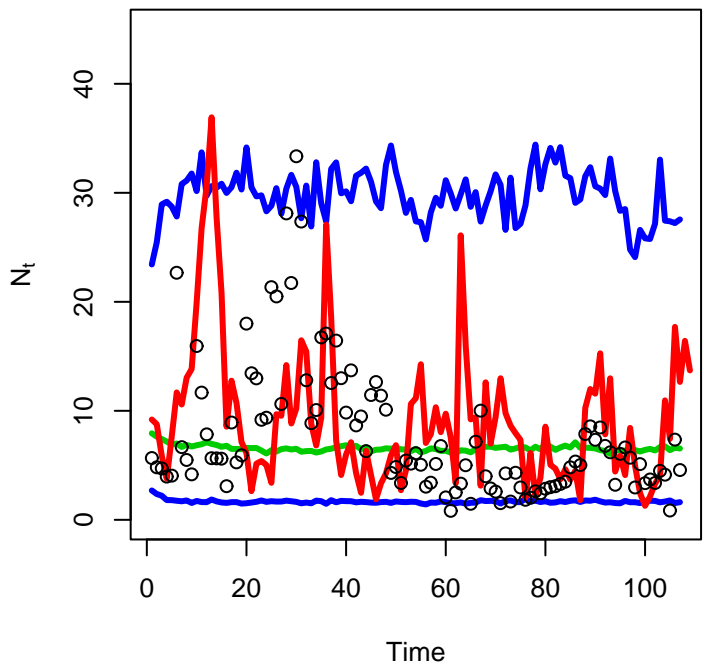
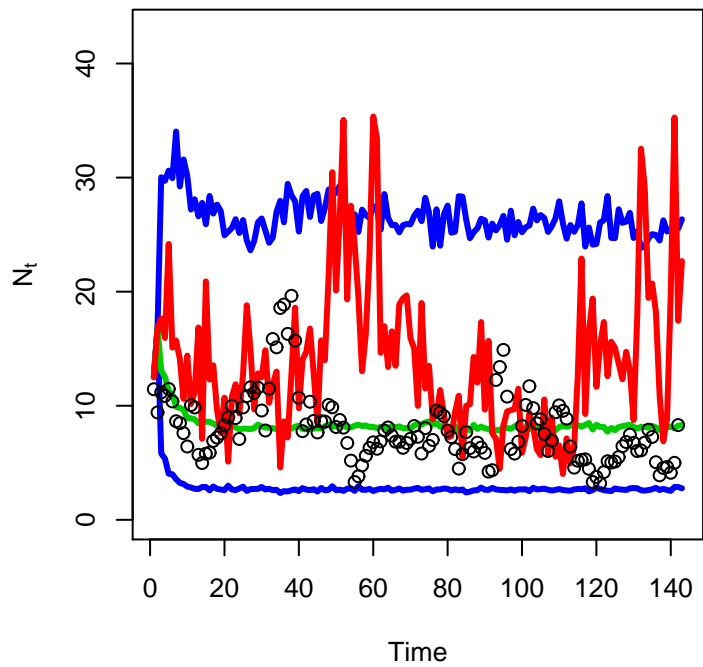


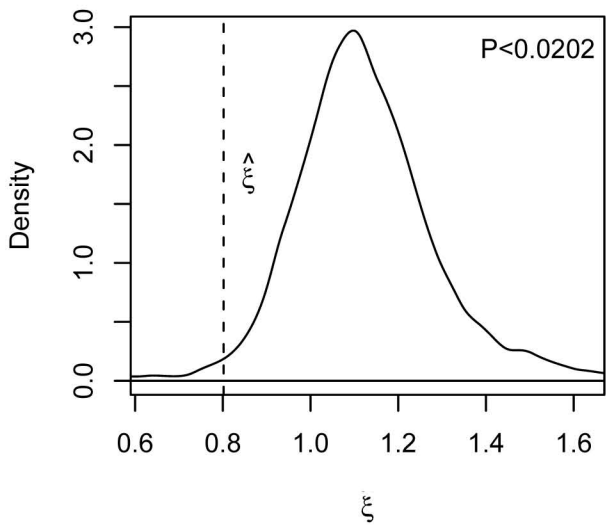
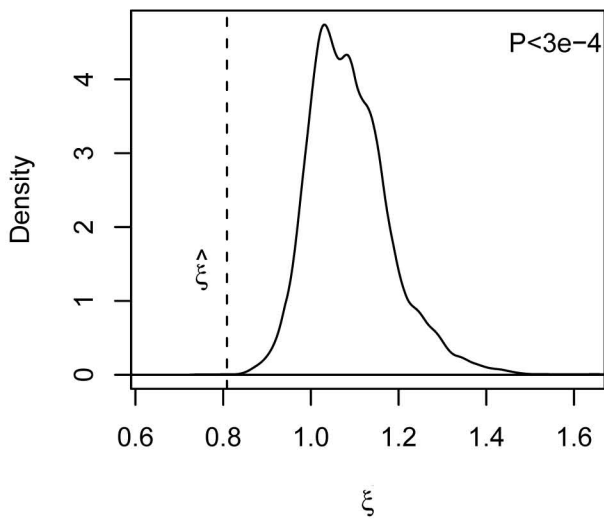
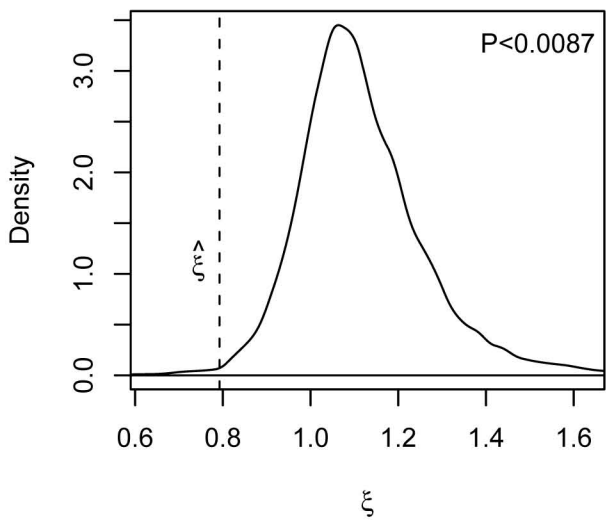
Phase





A**B****C****D**

A**B****C****D**

A**B****C****D**